The Urinary Tract: Renal Collecting Systems, Ureters, and Urinary Bladder

21

Keith P. Tomich and Sherif G. Nour

Introduction

It is useful for the purpose of this chapter to divide the urinary tract into two anatomic categories: the *upper urinary tract,* comprised of the renal collecting system and ureter, and the *lower urinary tract*, comprised of the urinary bladder and urethra. Even though the upper and lower urinary tract represent one contiguous anatomical area and are affected by many common pathological conditions, using a location-based approach to abnormal findings often helps tailor one's differential diagnosis.

We will first outline the normal anatomy of the upper urinary tract, necessary for every radiologist to understand before being able to identify potential pathology. We will examine some of the most common entities encountered in practice—urinary obstruction and urolithiasis—while also considering other less common but important pathology such as urothelial carcinoma.

K.P. Tomich, MD (✉)
Department of Radiology,
Kaiser Permanente Georgia Region,
Atlanta, GA, USA
e-mail: ktomich@gmail.com; keith.p.tomich@kp.org

S.G. Nour, MD, FRCR
Department of Radiology and Imaging Sciences,
Emory University Hospitals
and School of Medicine, Atlanta, GA, USA
e-mail: sherif.nour@emoryhealthcare.org

Normal Anatomy

The normal urinary collecting system is typically comprised of 8–12 *renal calyces.* Each calyx receives excreted urine from its paired renal papilla and drains through a valveless *infundibulum* into the renal pelvis. The renal pelvis is situated medially within the renal sinus fat and funnels into the ureter at the *ureteropelvic junction (UPJ).*

The ureters typically exit the renal pelvis at the level of L2 or L3 and then course inferiorly, parallel to the spine, near the transverse processes. In supine patients (as in most axial imaging acquisitions), the ureters typically fall dependently to rest—at least in part—on the psoas muscles. At the pelvic inlet, the ureters may turn slightly laterally before curving sharply toward the bladder trigone, entering at roughly 45° angle with respect to the bladder. The short tunneled segment of the ureter within the bladder wall is termed the *ureterovesicle junction (UVJ).*

It should be noted that radiologists and urologists may use the terms "proximal ureter," "midureter," and "distal ureter" differently when localizing an abnormality. Many radiologists are accustomed to dividing the ureteral length into equal thirds for this determination. On the other hand, urologists divide the ureter into three unequal segments based on anatomic landmarks. In this case, the *proximal ureter* is the longest segment between the UPJ and the superior edge of the sacrum. *Midureter* is the segment spanning the sacrum. *Distal ureter* is the shortest segment from the sacral tip to the bladder.

The entire upper urinary tract including the renal collecting system and ureter is lined by a single layer of transitional epithelium, i.e., *urothelium.*

K.M. Elsayes (ed.), *Cross-Sectional Imaging of the Abdomen and Pelvis: A Practical Algorithmic Approach*,
DOI 10.1007/978-1-4939-1884-3_21, © Springer Science+Business Media New York 2015

Imaging Approach

Traditionally, imaging of the upper urinary tract has been accomplished through intravenous pyelography (IVP), a serial radiographic examination that provides high resolution lumenography but is otherwise limited in characterization of intrinsic urothelial lesions, surrounding anatomy, and potential extrinsic abnormalities.

Ultrasound continues to provide an excellent adjunct to screen for hydronephrosis but lacks sensitivity for detection of small neoplasms. Ultrasound may successfully demonstrate stones within the renal collecting system, but is inadequate for imaging of all but the most proximal and distal segments of the ureters.

Advances in multidetector CT (MDCT) have allowed the development of high resolution CT for stone detection and CT urography (CTU), which have largely replaced the role of radiography and IVP in routine urologic practice. Additionally, MR urography (MRU) now allows imaging of the urinary tract using gadolinium-enhanced MR excretory urography or utilizing the intrinsic T2 signal of the fluid-filled urinary tract. MR also avoids the risks of iodinated contrast, especially problematic in patients with coexisting impaired renal function, and ionizing radiation.

Hydronephrosis

Dilatation of the renal collecting system is easily recognized by ultrasound, CT, or MR as abnormal enlargement of the renal pelvis and calyces. When dilated, the renal pelvis typically bulges anteriorly and medially with respect to the renal sinus. Additionally, as the pelvis and calyces expand within the renal sinus, there is obliteration of the renal sinus fat. Morphologic changes also occur: calyceal "blunting" in milder cases and calyceal "clubbing" in more severe cases. As parenchymal pressure builds within the kidney, stranding develops in the perinephric fat, thought to be secondary to lymphatic obstruction [1]. Algorithm 21.1 illustrates diagnostic approach for evaluation of urinary tract dilatation.

UPJ Obstruction

Obstruction of the ureteropelvic junction (UPJ) is the most common congenital cause of hydronephrosis. The pathogenesis of UPJ obstruction is not fully understood, but congenital UPJ obstruction is most likely an intrinsic muscular

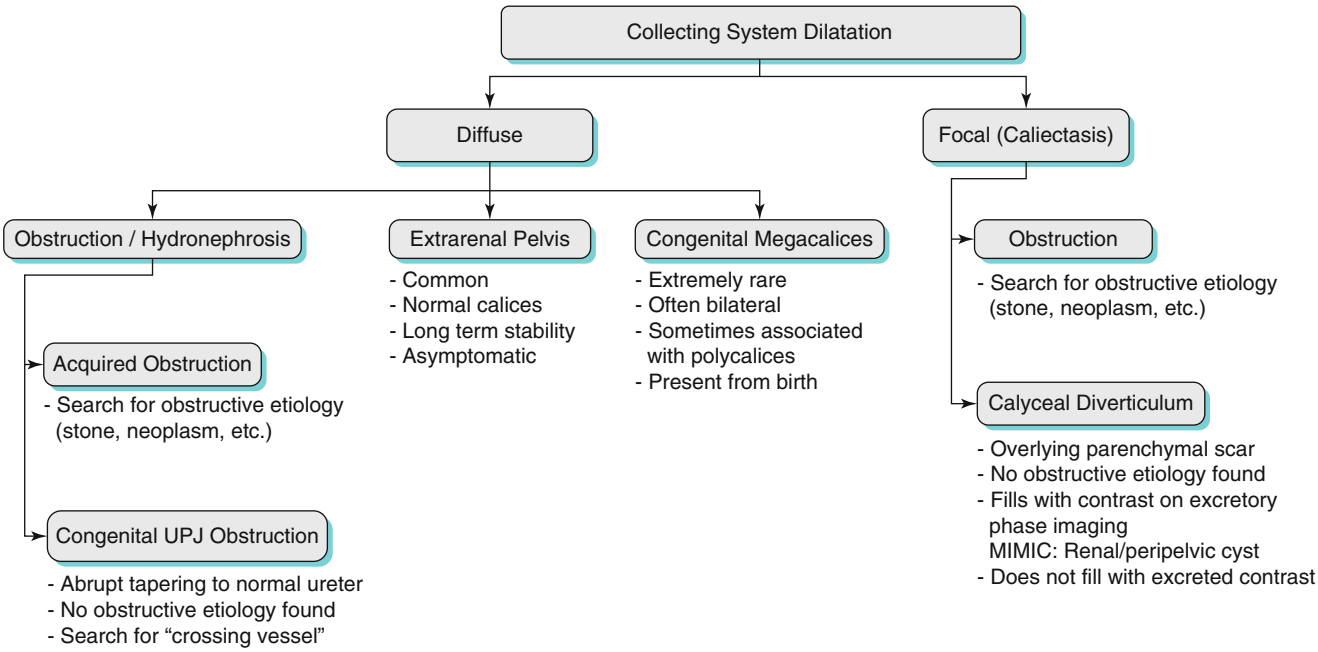

Algorithm 21.1 Decision tree detailing the evaluation of collecting system dilatation

deficiency, resulting in failed relaxation at the UPJ [2], somewhat analogous to achalasia of the esophagus.

The so-called crossing vessels have also been implicated in UPJ obstruction. In this case, when a patient is found to have UPJ obstruction, investigation may reveal a retroperitoneal artery or vein crossing anterior to the ureteropelvic junction, producing at least a visual sensation in some cases that the crossing vessel is actually causing the obstruction by extrinsic compression (Figs. 21.1, 21.2, and 21.3). However, these "crossing vessels" are also found in normal individuals and their functional significance in patients with UPJ obstruction is therefore controversial [2]. Nevertheless, crossing vessels are important to define in patients with UPJ obstruction in whom surgical correction (endopyelotomy) is contemplated, given the increased risk of retroperitoneal hemorrhage [3].

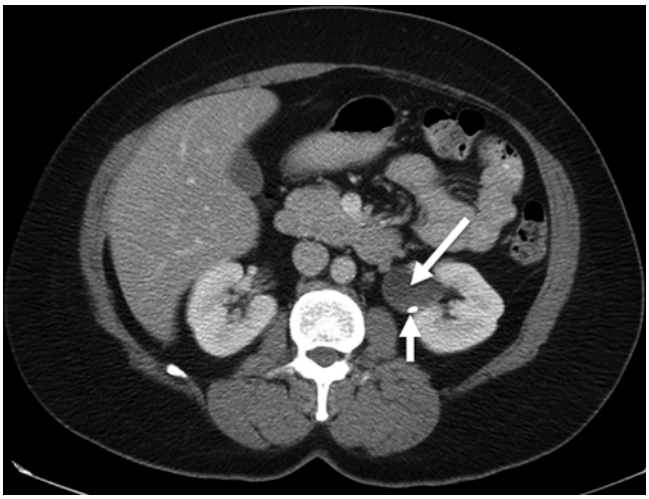

Fig. 21.1 Extrarenal pelvis. Nephrographic phase CECT. Dilated left extrarenal pelvis (*long arrow*) containing a small, nonobstructing calculus (*short arrow*)

Extrarenal Pelvis

Variations in position and shape of the renal pelvis are common and can mimic obstructive uropathy. When situated outside the renal sinus, the renal pelvis is unconfined by solid renal parenchyma and consequently may appear bulbous and dilated, even when unobstructed. Extrarenal pelves are occasionally difficult to distinguish from mild cases of ureteropelvic junction obstruction since the ureter is normal caliber in both conditions (Figs. 21.4 and 21.5). However, identification of normal decompressed calyces favors a diagnosis of extrarenal pelvis. When the diagnosis remains in doubt, especially in pediatric patients, functional imaging using radionuclide renography is often utilized to help exclude UPJ obstruction.

Congenital Megacalycosis

Congenital megacalycosis (CM) is a very rare developmental anomaly caused by hypoplasia or failed development of the renal medullary pyramids [4]. The condition is

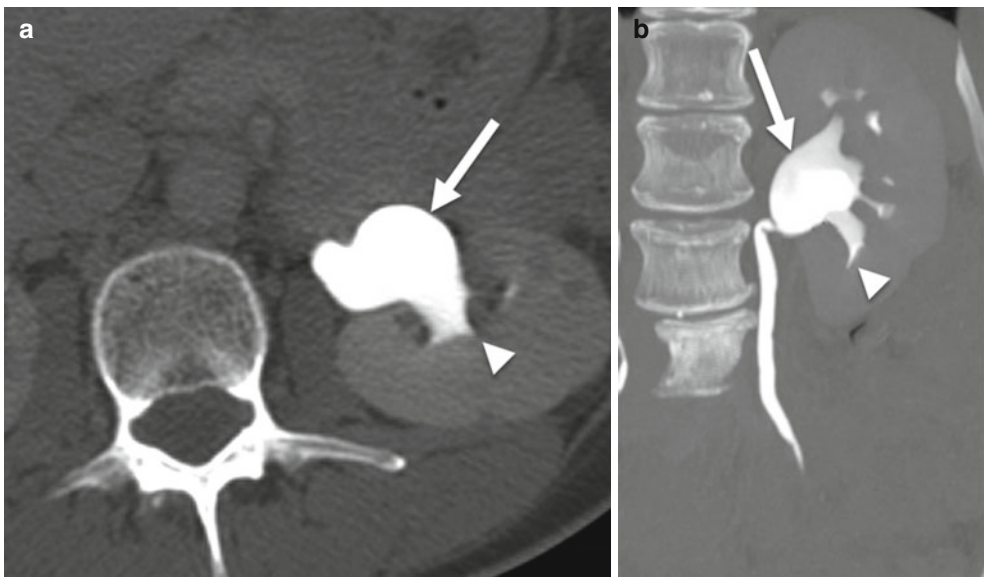

Fig. 21.2 Extrarenal pelvis. Axial (**a**) and coronal maximum intensity projection (**b**) excretory phase CT urogram. Dilated renal pelvis (*arrows*) but sharp renal calyces (*arrowheads*) and normal ureter

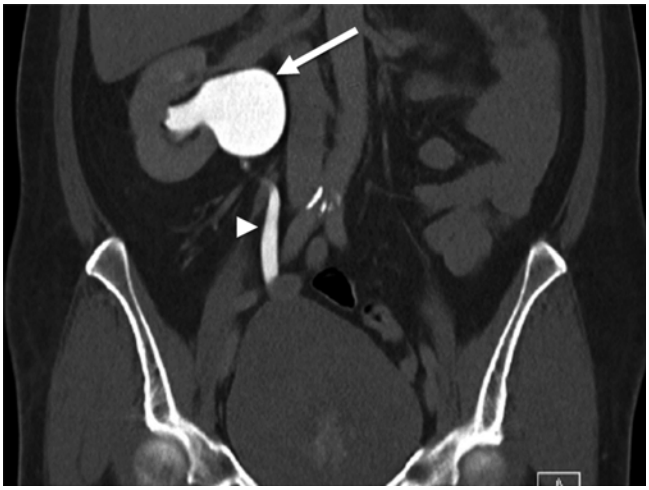

Fig. 21.3 Ureteropelvic junction obstruction. Coronal excretory phase CECT. Markedly dilated right renal pelvis (*arrow*) with normal caliber proximal ureter (*arrowhead*)

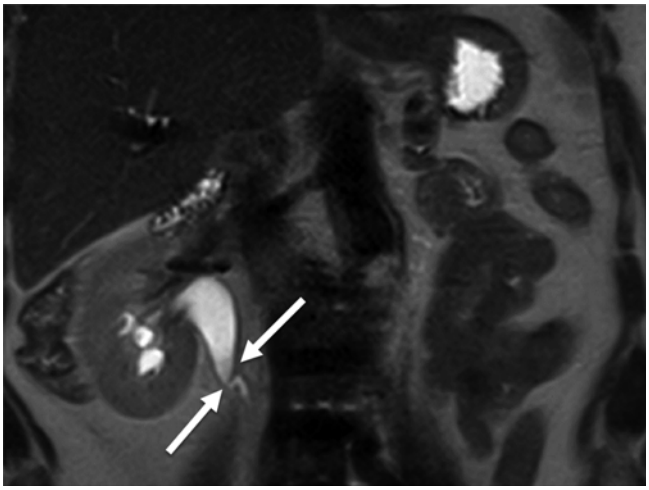

Fig. 21.5 Ureteropelvic junction obstruction. Coronal T2-weighted MR. Right pelvicaliectasis with rapid tapering at the ureteropelvic junction (*arrows*) to normal caliber ureter

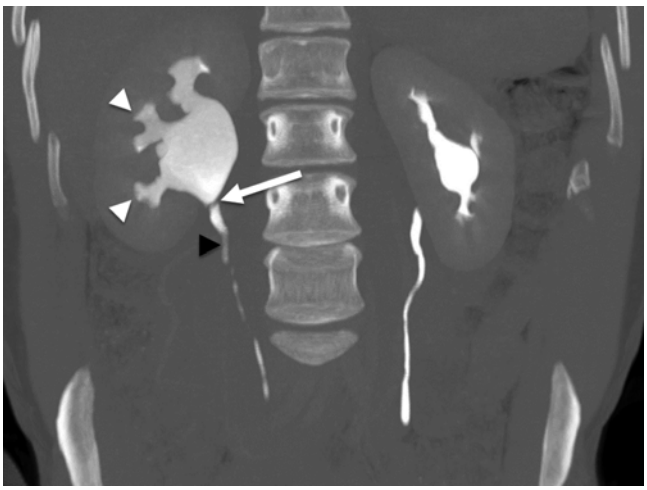

Fig. 21.4 Ureteropelvic junction obstruction. Coronal MIP CT urogram. Marked right calyceal dilation and blunting (*white arrowheads*) and dilated right renal pelvis, with rapid tapering at the ureteropelvic junction (*white arrow*) to normal caliber ureter (*black arrowhead*). Normal left renal collecting system and ureter

characterized by (1) an *increased number* of (2) *oversized* renal calyces (Fig. 21.6). This entity can be distinguished from hydronephrosis and congenital UPJ obstruction in that the size of the renal pelvis and ureter in CM is normal.

Complications of CM include formation of renal calculi and recurrent urinary tract infections [5], either of which may precipitate discovery of the condition.

Calyceal Diverticulum

A calyceal diverticulum is a cyst-like lesion of the renal parenchyma but is differentiated from a true renal cyst by the presence of a communication with the renal collecting system. Most calyceal diverticula are likely congenital in etiology, while a minority may be sequelae of prior infection or stone disease (Fig. 21.7). Most commonly, calyceal diverticula are found at the upper pole of the kidney in relation to a minor calyx and typically rather small. Less common is a diverticulum found in the central interpolar region of the kidney in relation to a major calyx or the renal pelvis. These tend to be quite large [6].

Like any site of urinary stasis, calyceal diverticula can harbor infection and stone formation. Calyceal diverticula are easily distinguished from renal cysts by excretory phase imaging: calcyceal diverticula opacify with contrast, whereas renal cysts do not. Even a shallow contrast pool within a cystic structure is considered pathognomonic.

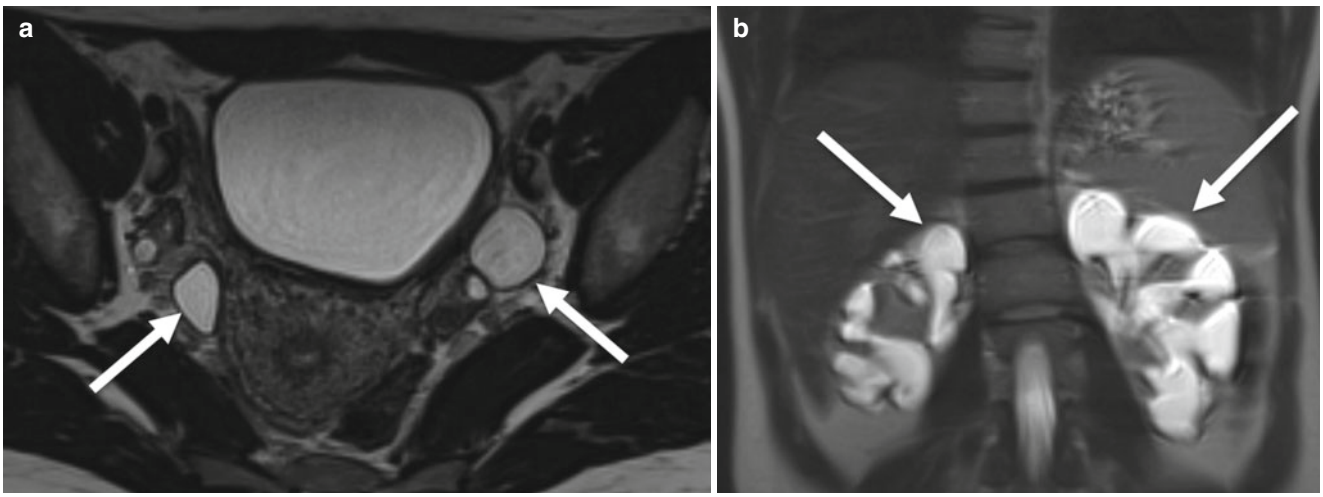

Fig. 21.6 Congenital megaureter with megacalyces. Axial (**a**) and coronal (**b**) T2-weighted MR. (**a**) Bilateral markedly dilated distal ureters (*arrows*). (**b**) Bilateral markedly dilated renal calyces (*arrows*)

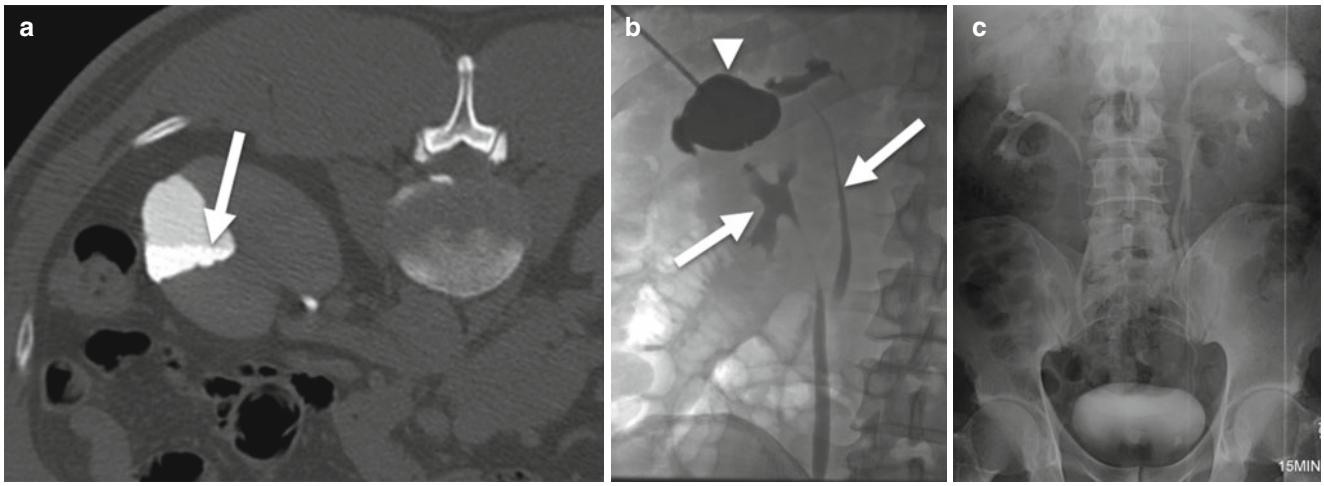

Fig. 21.7 Calyceal Diverticulum. (**a**) Axial prone excretory phase CT urogram. Contrast-opacified, triangular parenchymal defect. Note fluid-fluid level resulting from layering contrast material within stagnant urine (*arrow*). (**b**) Antegrade nephrostagram. Direct contrast injection of diverticulum (*arrowhead*) with subsequent filling of a duplicated collecting system (*arrows*). (**c**) Intravenous pyelogram

Obstructive Uropathy

Urinary obstruction is one of the most common urologic entities encountered in clinical practice and radiology. Obstruction is seen in all age groups and the causes are numerous, both congenital and acquired and benign and malignant. Among these, the vast majority of cases are acquired benign conditions—mostly urolithiasis.

Cases of chronic urinary obstruction may go unnoticed by the patient for many years, even when severe. When given time to accommodate, the renal pelvis and ureter may balloon to massive size without sequelae of infection, inflammation, or rupture. However, chronic urinary stasis does favor stone formation and infection. The natural course of unrecognized or untreated hydronephrosis is renal parenchymal damage, progressing to renal atrophy and loss of renal function.

On the other hand, acute obstruction, even when causing only mild hydronephrosis, can present with severe symptoms of renal colic and flank pain but little (if any) measurable change in renal function. Acute obstruction may be complicated by *forniceal rupture* with retroperitoneal leakage of urine (Figs. 21.8 and 21.9).

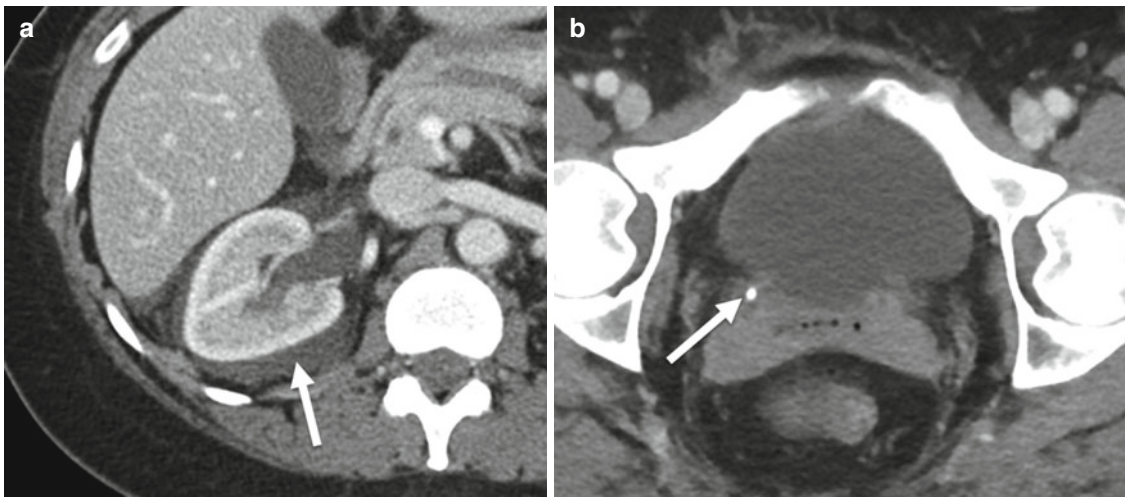

Fig. 21.8 Forniceal rupture. Axial corticomedullary phase CECT. (**a**) Right perinephric and peripelvic fluid (*arrow*) but relatively decompressed renal collecting system, signifying forniceal rupture secondary to (**b**) obstructing calculus at the ureterovesicle junction (*arrow*)

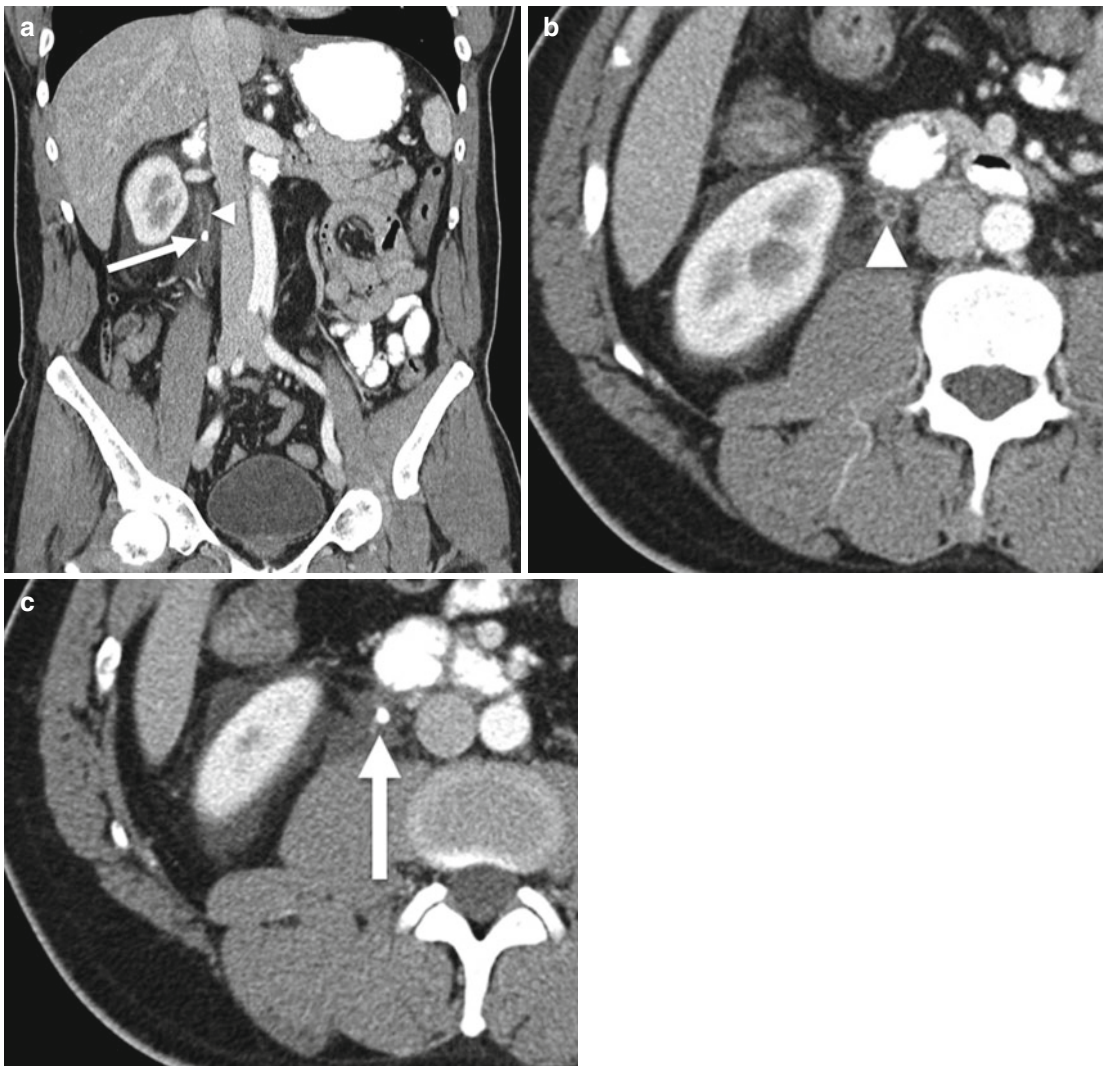

Fig. 21.9 Forniceal rupture. Coronal (**a**) and axial (**b**, **c**) corticomedullary phase CECT. Obstructing stone within the right proximal ureter (*arrows*). Upstream urothelial enhancement consistent with reactive inflammation (*arrowhead*). Perinephric and periureteral fluid suggestive of forniceal rupture

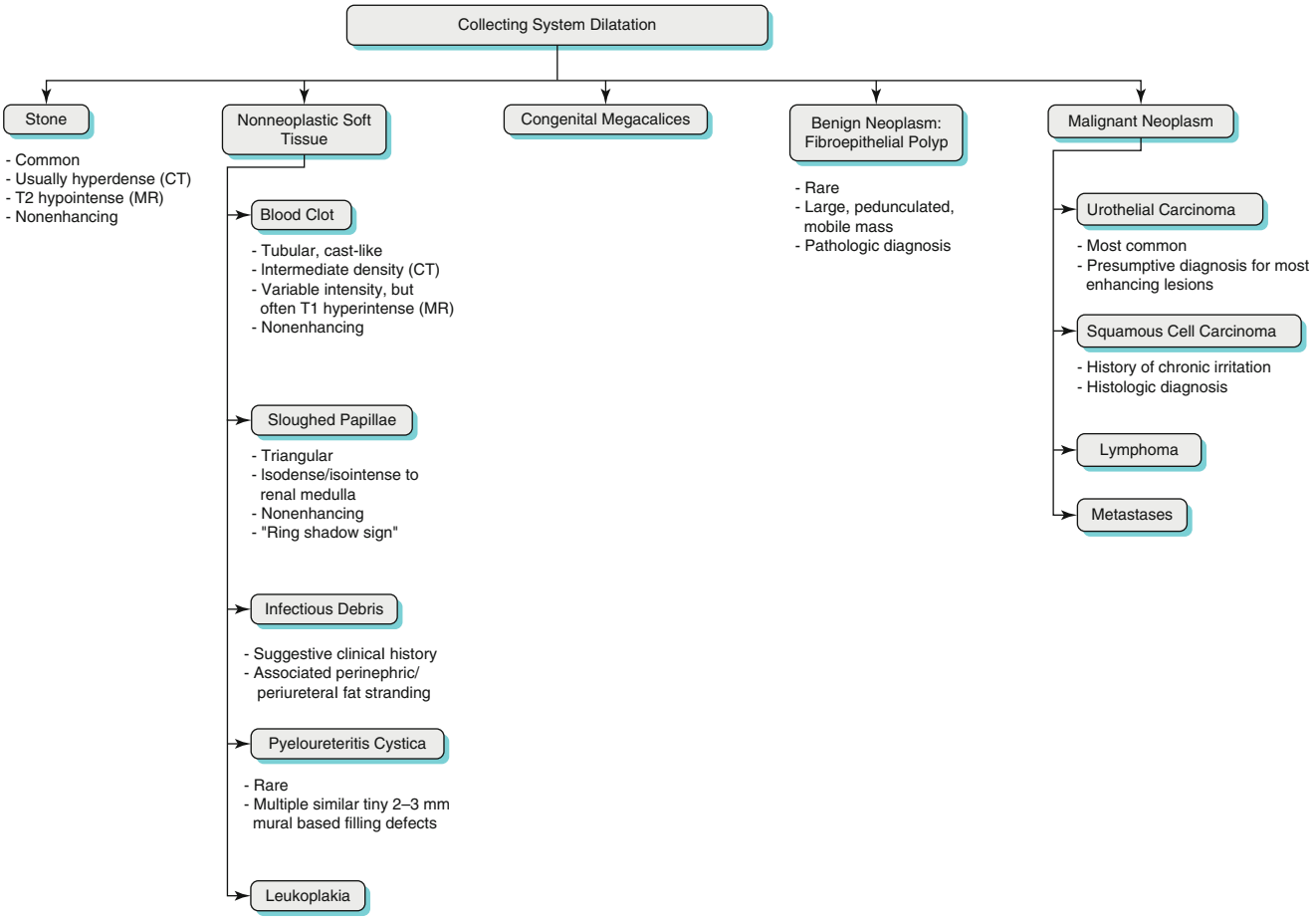

Algorithm 21.2 Systematic approach to determining the etiology of filling defects in the upper urinary tract

Various causes can lead to the visualization of filling defect within the urinary tract. Algorithm 21.2 illustrates common etiologies for filling defects within the urinary tract.

Urolithiasis

Traditional radiography remains relatively sensitive (up to 85 %) in detection of urinary stones, because most stones contain calcium. However, identification of stones on radiographs is often hampered in patients of large body habitus and confounded in patients with non-urinary calcifications, such as vascular phleboliths.

On the other hand, by adding the ability to identify non-calcium stones (uric acid, xanthine, and cystine), MDCT raises the sensitivity for stone detection up to 98 % [7]. Only pure matrix stones and indinavir stones are likely to be missed at noncontrast CT because they are of soft tissue attention, although secondary changes of obstruction may imply their presence anyway [7].

Most calculi within the renal collecting system are too small to cause obstruction, and many are often discovered incidentally on CT imaging performed for other indications. Nevertheless, careful attention is warranted to the "incidental" stone, as the findings of local obstruction of a single urinary calyx may be quite subtle. Comparison with adjacent normal calyces or with the contralateral normal kidney may help confirm localized caliectasis. Besides dilatation, secondary imaging findings of urinary obstruction mimic those of infection and inflammation: stranding of the periureteral and perirenal fat.

Urinary calculi naturally lodge at the anatomic points of narrowing along the urinary stream, namely, (from proximal to distal) the calyceal-infundibular junction, the ureteropelvic junction, the ureterovesicle junction, and the bladder neck.

Sloughed Papillae

A sloughed papilla refers to the detached papillary tip that occurs after ischemic necrosis. The renal medulla and especially the papillary tips are vulnerable to ischemia from any cause, but common causes include diabetes mellitus, analgesic/NSAID abuse, renal vein thrombosis, sickle cell disease, and hypotensive shock. Once detached, sloughed papillae may be seen as noncalcified and nonenhancing filling defects in the

renal pelvis. On excretory phase imaging, a triangular filling defect may be seen surrounded by a thin rim of contrast material, referred to as the "ring-shadow sign." Like any mobile filling defect, sloughed papillae can migrate into the ureter, resulting in obstruction with urinary colic, or pass distally without complication or symptoms. Old sloughed papillae may calcify, thus representing a rare cause of urinary calculi.

Sloughed papillae are occasionally distinguished from other soft tissue filling defects by their classic triangular shape. Unlike urothelial carcinoma, sloughed papillae do not enhance.

Blood Clot

Renal hemorrhage with clot retention in the ureter is an important but uncommon cause of urinary obstruction. Typically, renal hemorrhage in these cases is caused by trauma, including accidental blunt trauma, such as a motor vehicle collision, as well as iatrogenic trauma, such as hematuria following percutaneous renal biopsy or nephrostomy. Bleeding caused by a proximal urothelial carcinoma may also result in obstructive ureteral blood clots.

Ureteral blood clots can be distinguished from other ureteral filling defects by certain features. Blood clots typically form elongated or "tubular" filling defects, producing a "finger-in-glove"-like appearance when surrounded by excreted contrast media. Blood clots may appear of various density based on age and concentration of blood products but do not show enhancement following contrast administration.

Pyeloureteritis Cystica

Pyeloureteritis cystica is a benign condition characterized by subepithelial cysts that elevate the mucosal lining of the renal pelvis and/or ureter [8]. The condition is most commonly found in the proximal ureter (*ureteritis cystica*) but may also involve the renal pelvis *(pyelitis cystica)*. As its name implies, pyeloureteritis cystica is thought to be related to chronic infection or inflammation, as seen with chronic urinary tract infection or chronic stone irritation. In and of itself, pyeloureteritis cystica is asymptomatic and considered an incidental imaging finding, though the causative process may be symptomatic.

Pyeloureteritis cystica is characterized on imaging by multiple small (2–5 mm), round, smooth-walled, eccentric filling defects protruding from the wall of the renal pelvis or ureter (Fig. 21.10). Although excretory phase imaging may show narrowing of the involved lumen, frank obstruction by submucosal cysts is very rare. The condition is usually stable over time and imaging follow-up is not routinely recommended. Pyeloureteritis cystica is not considered a premalignant condition, though it is controversial whether patients are at increased risk for development of urothelial carcinoma [8].

Leukoplakia and Malakoplakia

Leukoplakia is an uncommon lesion of the urothelium resulting from squamous metaplasia in the setting of chronic

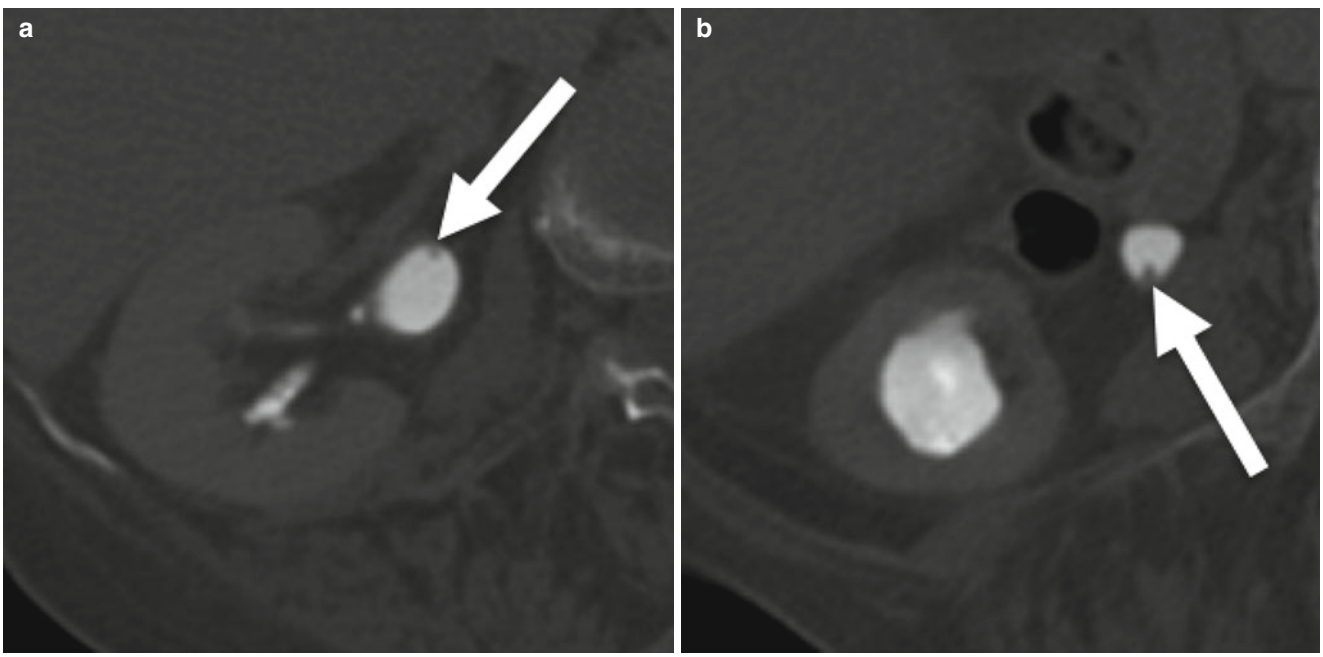

Fig. 21.10 Ureteritis cystica. Axial excretory phase CT urogram at the level of the renal pelvic (**a**) and progressing down the ureter (**b**-**e**). Multiple tiny (2–3 mm) filling defects arising from the walls of the right renal pelvis and ureter (*arrows*)

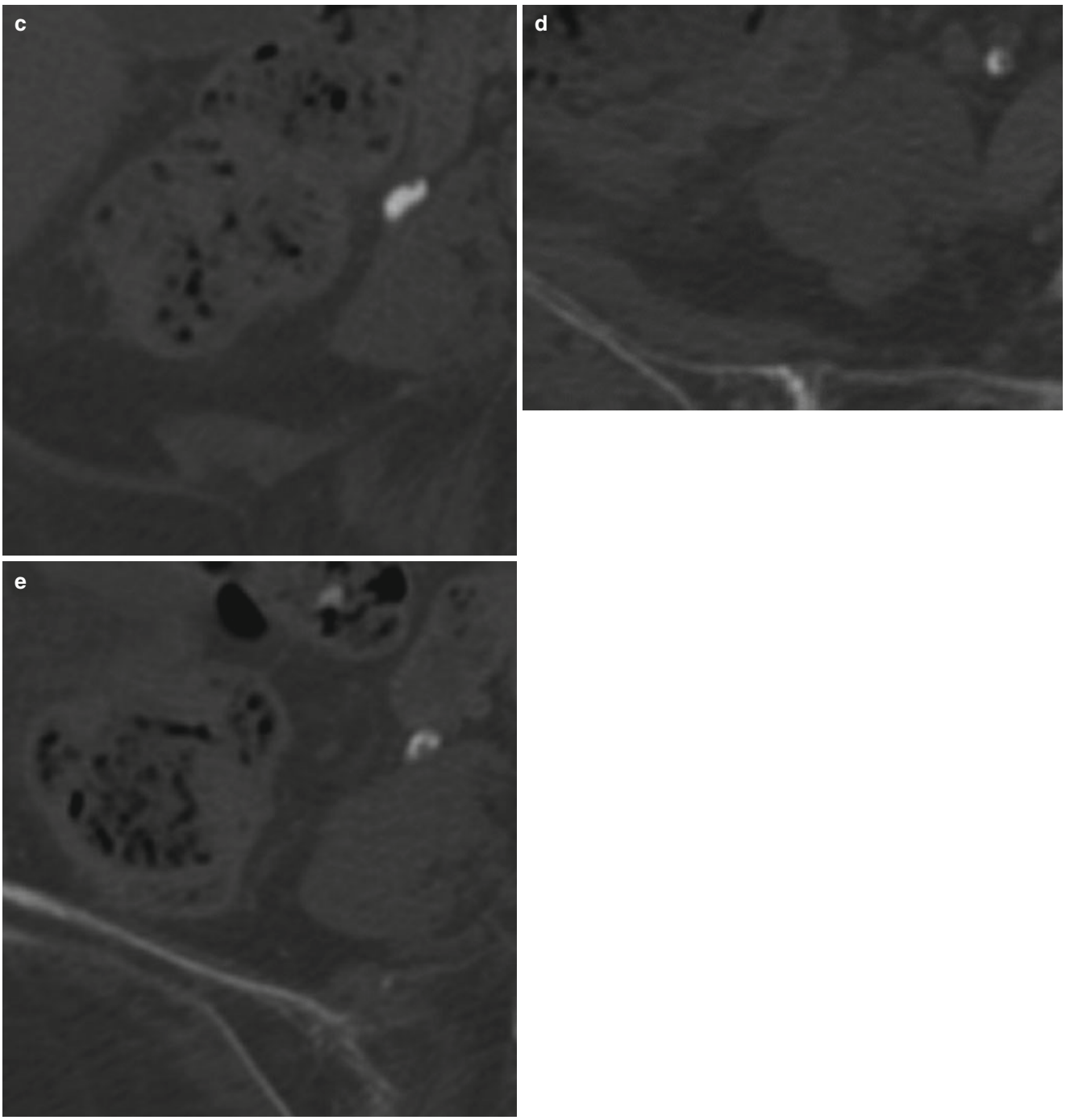

Fig. 21.10 (continued)

inflammation. Leukoplakia is characterized by plaque-like mural based filling defects which may be indistinguishable from urothelial carcinoma. Unlike pyeloureteritis cystica, leukoplakia is considered a premalignant lesion along the spectrum of development of squamous cell carcinoma. Indeed, when leukoplakia is found at one site in the urinary tract, a synchronous squamous cell carcinoma is often present.

Malakoplakia is another cause of a plaque-like filling defect in the upper urinary tract. However, malakoplakia represents a granulomatous reaction to chronic inflammation and is not considered a premalignant lesion [9]. Nevertheless, imaging differentiation of leukoplakia and malakoplakia from urothelial carcinoma is virtually impossible and tissue sampling is typically recommended.

Benign Neoplasms: Fibroepithelial Polyp

Most ureteral neoplasms are malignant and epithelial in origin, i.e., urothelial carcinoma. Conversely, a *fibroepithelial polyp* is of mesodermal origin and is the most common benign neoplasm of the ureter, yet fewer than 200 cases have been reported in the literature [10]. Fibroepithelial polyps are more common in adults ranging 20–40 years of age, but have also been found in children. They are usually solitary and most commonly found in the proximal ureter [11]. Excretory imaging demonstrates a smooth, slender, elongated filling defect ranging in size from 1 to 5 cm, though occasionally longer than 10 cm [10]. Because of their usual pedunculated attachment, they can appear as mobile ureteral masses and result in intermittent obstructive uropathy. Nevertheless, hematuria is a more common presentation than renal colic.

Malignant Neoplasm

Compared to tumors of the kidney and bladder, primary neoplasms of the renal pelvis and ureter are rare. In total, they account for only 5 % of all neoplasms of the urinary tract diagnosed each year [12]. Unfortunately, the vast majority of these tumors are malignant, with 85–90 % representing transitional cell carcinoma (TCC), now preferably termed *urothelial carcinoma* (UC) [12]. Squamous cell carcinoma accounts for an additional 10 % of upper urinary tract malignancies, usually resulting from squamous metaplasia occurring secondary to chronic irritation. Indeed, more than half of the patients with squamous cell carcinoma of the ureter also have urinary calculi [13]. Other histologies of upper urinary tract malignancy are extremely rare, including adenocarcinoma which accounts for less than 1 % of cases.

Certain chemical carcinogens—notably phenacetin—excreted in the urine are implicated in the pathogenesis of urothelial carcinoma and squamous cell carcinoma. This is thought to be due to the concentration and prolonged exposure that occurs along the urinary tract. Like urinary bladder cancer, males are twice more commonly affected than females [13].

By location, urothelial carcinoma of the upper urinary tract occurs most frequently in the extrarenal portion of the renal pelvis, followed by the calyceal-infundibular junction (Figs. 21.11 and 21.12). Ureteral UC is less common, accounting for only 25 % of cases. Approximately 60–75 % of cases of ureteral UC involve the distal third of the ureter [7, 8]. It is important to recognize that urothelial carcinoma has a propensity for multicentric disease: Synchronous bladder cancer is found in 2–4 % of patients with upper tract tumors, while metachronous bladder cancer will develop in 40 % of these patients [14]. Hence, detailed evaluation of the entire urinary tract is warranted at primary staging and surveillance imaging, especially during the first 24 months of surveillance when a majority of new lesions will develop [13].

Lesions in the renal pelvis (Figs. 21.13 and 21.14), like those in the urinary bladder, classically grow as a polypoid mass protruding into the lumen. When surrounded by contrast media on excretory phase CT or MRI or by T2 hyperintense urine on MRI, a classic polypoid filling defect is seen. However, even a small lesion involving a calyx or infundibulum may entirely plug the lumen such that no opacification occurs and no filling defect is depicted, resulting in the so-called phantom calyx [15]. Portal venous phase imaging can help in this instance, as any tumor filling the "phantom calyx" should enhance with contrast.

Due to its relatively narrow lumen, ureteral carcinomas are uncommonly seen as classic polypoid masses. Instead, these lesions tend to produce nonspecific soft tissue filling defects with or without surface irregularity [15]. The only sign in some cases may be a focal point of obstruction resulting in proximal hydroureteronephrosis. However, most patients present with hematuria before frank urinary tract obstruction. If these neoplasms form strictures, as they commonly will in the ureter, they may be circumferential or eccentric. They are often markedly irregular, a key differentiating feature from benign strictures. If smooth, clues to malignancy include non-tapering ("shouldered") margins.

Multiphasic CT with CT urography is the current gold standard for imaging evaluation and characterization of urothelial carcinoma. However, MRI is gaining greater acceptance, particularly for its rendering of soft tissue contrast, in patients where use of iodinated contrast is contraindicated. CT urography with adequate ureteral distention and opacification allows detection of early localized disease, affording patients an increased likelihood of less extensive, curative, surgical options [15].

According to Browne et al., "TCC has lower signal intensity than the normally high-signal-intensity urine on T2-weighted images, permitting good demonstration of tumor in a dilated collecting system. However, TCC is nearly isointense to renal parenchyma on T1- and T2-weighted images, meaning that gadolinium based contrast agents are necessary for accurate assessment of tumor extent. Although TCC is a hypovascular tumor, moderate enhancement is seen with gadolinium contrast material, although not to the same degree as renal parenchyma."

Various masses can surround the ureter. Algorithm 21.3 illustrates the most common periureteric masses.

Retroperitoneal Fibrosis

Retroperitoneal fibrosis is a rare entity with an estimated incidence of 1 in 200,000, most often found in middle-aged men [16]. The typical age range is 40–60, while men are

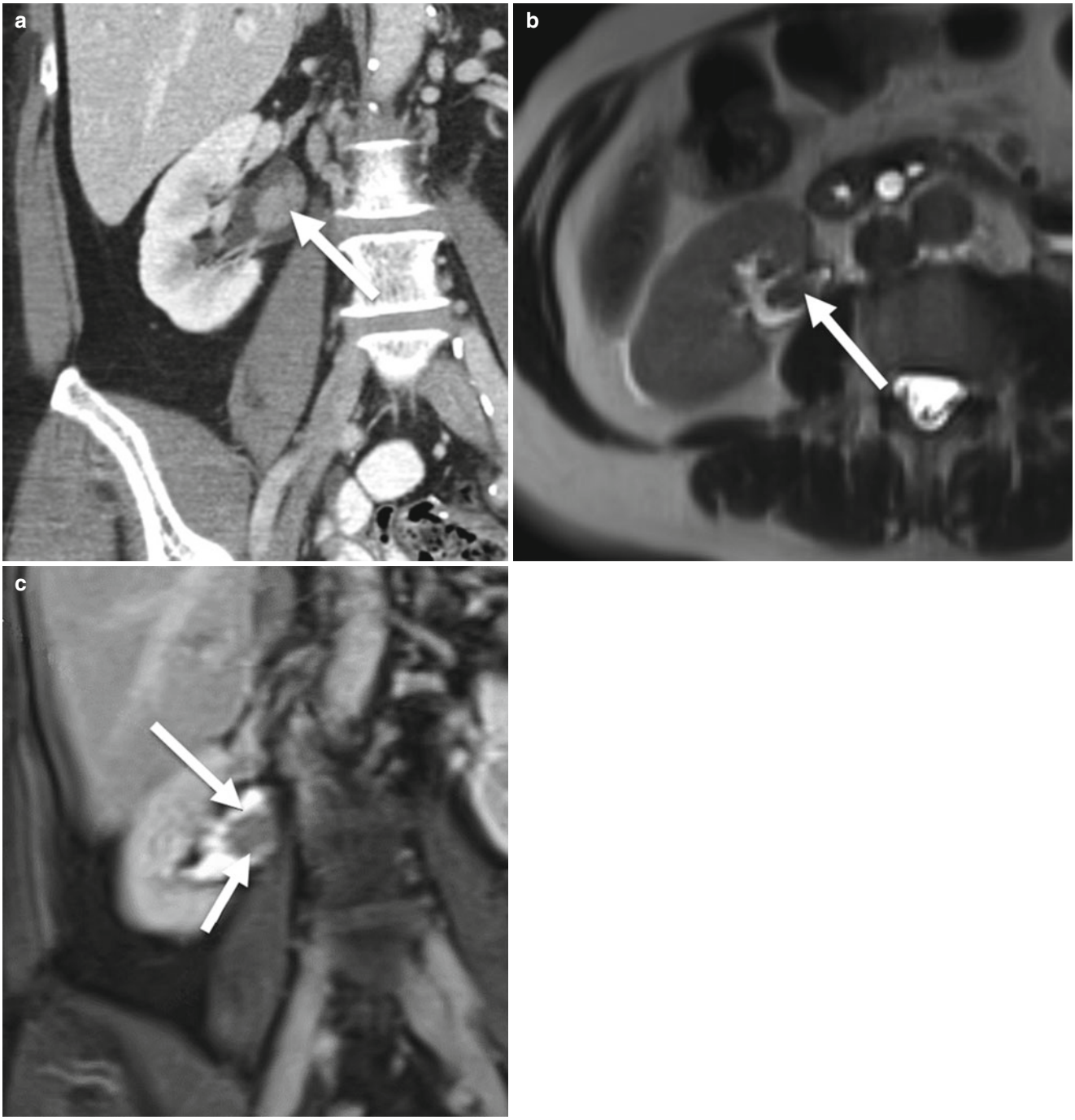

Fig. 21.11 Upper tract urothelial carcinoma. (**a**) Coronal nephrographic phase CECT. Enhancing soft tissue mass, right renal pelvis (*arrow*). (**b**) Axial T2-weighted MR. Intermediate to low signal filling defect, right renal pelvis (*arrow*). (**c**) Coronal T1+Gd. Enhancing soft tissue mass, right renal pelvis (*long arrows*). Histology showed urothelial carcinoma

affected two to three times more frequently than women [16]. Two thirds of cases of retroperitoneal fibrosis are considered primary or idiopathic, so-named Ormond's disease [17]. Remaining cases are secondary to primary insults such as external beam radiation, trauma or infection, and certain drugs including methysergide, ergotamines, hydralazine, and phenacetine.

Retroperitoneal fibrosis tends to present early as a mantle of soft tissue surrounding the distal aorta near the level of L4 and L5, often enveloping the aortic bifurcation and common iliac arteries. As tissue extends laterally, the ureters—often bilaterally—become encased and classically deviated medially by the retractile effect of the fibrotic tissue. Depending on stage, soft tissue may extend far superiorly

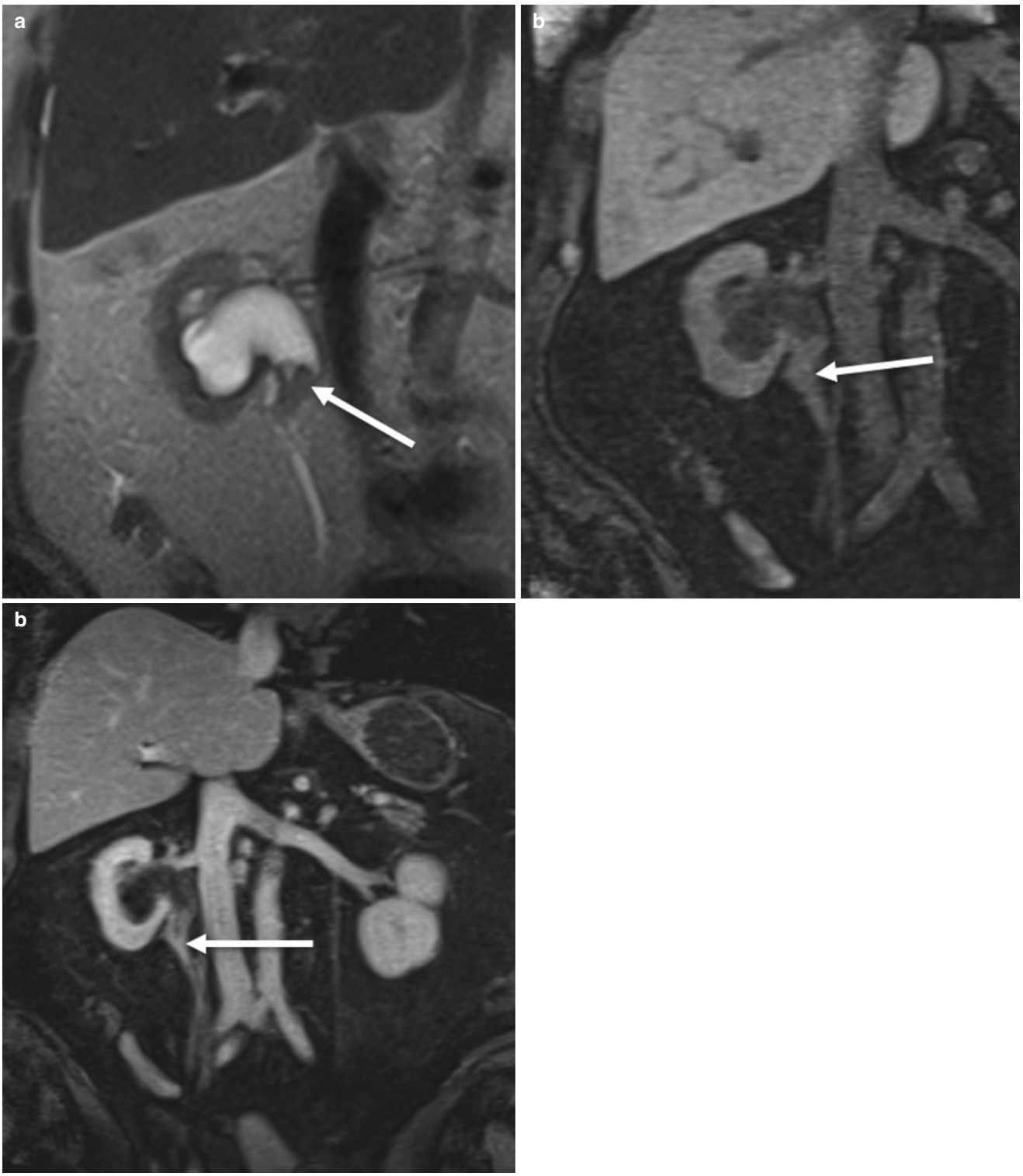

Fig. 21.12 Upper tract urothelial carcinoma. (**a**) Coronal T2-weighted MR. UPJ pattern obstruction with intermediate signal filling defect at right UPJ (*arrow*). (**b**, **c**) Coronal pre- and post-contrast T1. Enhancing soft tissue mass at right UPJ (*arrows*). Histology showed high grade urothelial carcinoma

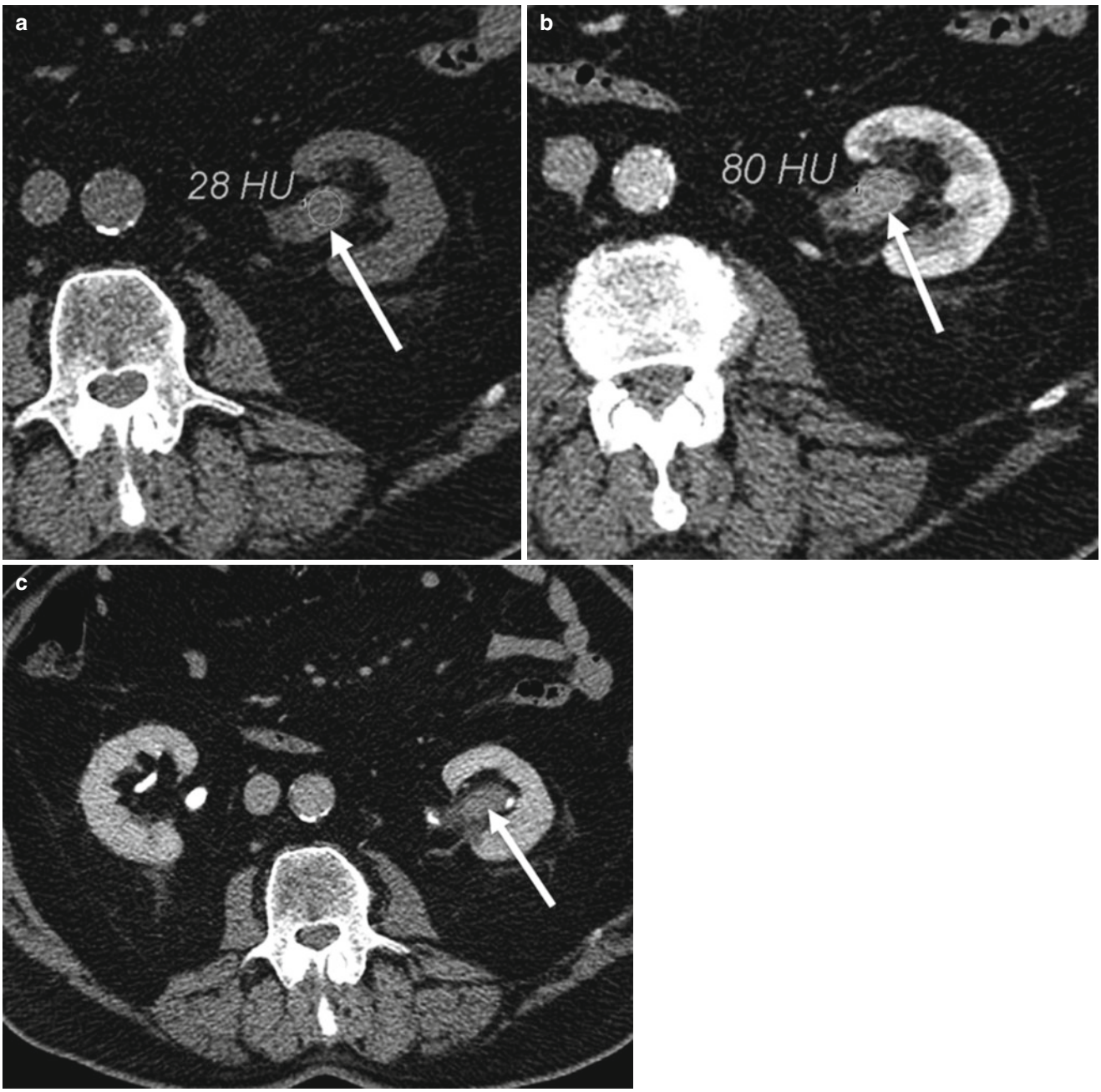

Fig. 21.13 Urothelial carcinoma. (**a**) Axial NECT. Vague abnormal soft tissue density in left renal pelvis (*arrow*). (**b**) Portal venous phase CECT. Enhancing soft tissue mass (*arrow*). Note the density measurements in Hounsfield units (HU) confirming enhancement (**a**, **b**). (c) Excretory phase CECT. Filling defect within left renal pelvis (*arrow*)

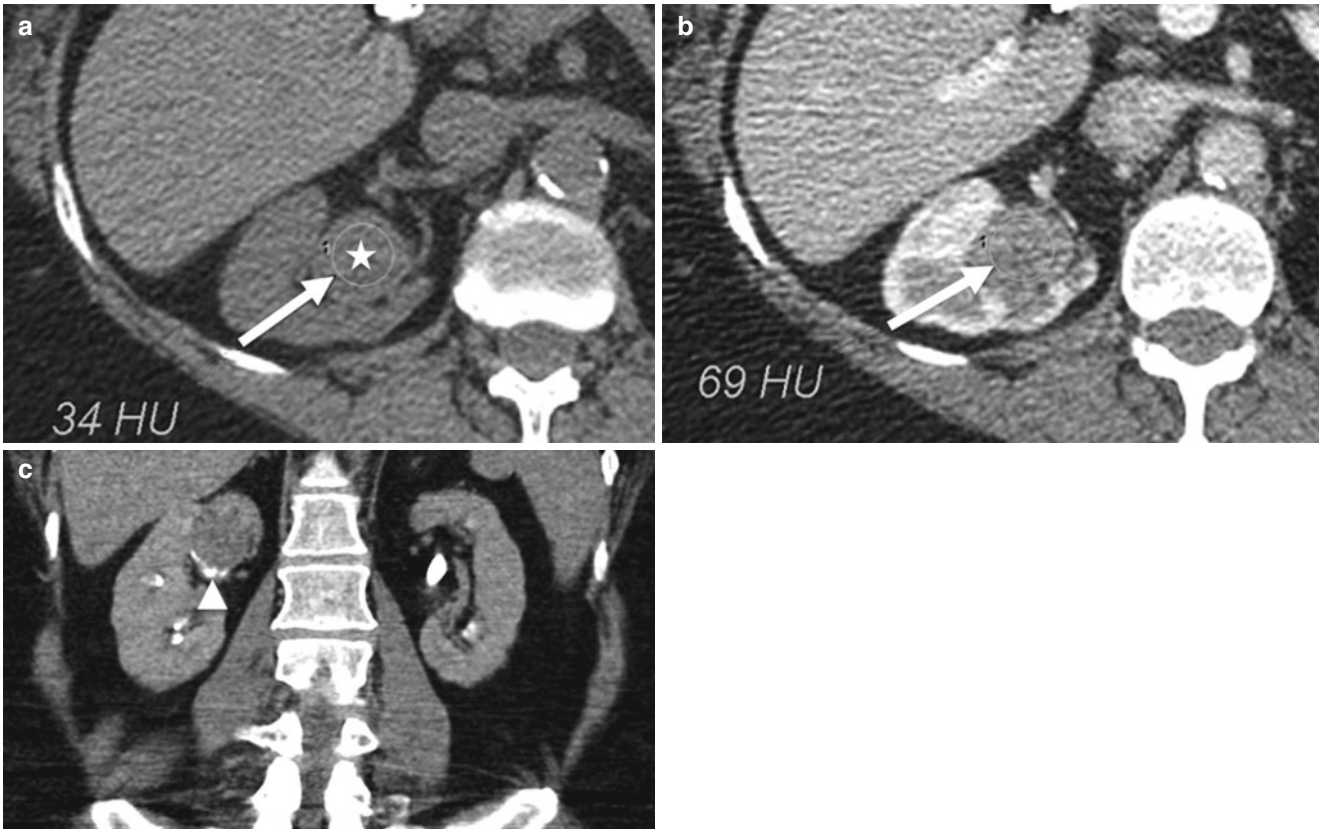

Fig. 21.14 Urothelial carcinoma. (**a**) Axial NECT with rounded soft tissue density distending an upper pole calyx (star). (**b**) Axial CECT confirms enhancement of this soft tissue mass. (**c**) Coronary excretory phase CT urogram. Round soft tissue filling defect within the right upper pole (*arrow*) with a claw of calyx at the inferior aspect of this lesion (*arrowhead*)

along the retroperitoneal axis to involve the duodenum, pancreas, and upper abdominal arteries (SMA, renal arteries, etc.). With more extensive disease, the ureters may become obstructed. Distinguishing benign retroperitoneal fibrosis from malignancy such as lymphoma is difficult and occasionally impossible. Nevertheless, benign retroperitoneal fibrosis tends to *encase* the aorta, IVC, and ureters, while lymphoma tends to encase and also *elevate* the aorta and IVC off the spine.

On CT, fibrotic soft tissue generally is isodense to muscle and demonstrates enhancement based on the disease activity: brisk enhancement may be seen with active inflammation while weak or no enhancement may be detectable in the chronic phase. Excretory phase imaging is appropriate in the setting of hydronephrosis, so that potential sites of ureteral obstruction can be localized.

On MR, fibrotic tissue tends to demonstrate low signal on T1- and T2-weighted imaging, except in the acute inflammatory phase when high signal on T2-weighted images may be seen reflecting edema. Dynamic postcontrast imaging with gadolinium generally mirrors T2 signal changes: early enhancement in the presence of active inflammation but weak delayed enhancement in the chronic indolent phase.

Lymphoma and Metastases

High on the "short list" of differential diagnoses for retroperitoneal masses are lymphoma and metastases. Urinary tract involvement by lymphoma and metastases are usually accompanied by generalized retroperitoneal disease, while isolated periureteral lymphoma and metastases are quite rare. Potential primary causes of periureteral metastases include primary neoplasms of the prostate, gastrointestinal tract, breast, and lung, as well as melanoma [18].

Lymphomatous involvement of the renal pelvis and ureter are usually found in the setting of direct lateral extension from adjacent retroperitoneal disease, less commonly from direct contiguous spread from renal and perirenal lymphoma (Fig. 21.15) [18]. Isolated peripelvic and periureteric lymphoma are very rare. Confident diagnosis of retroperitoneal

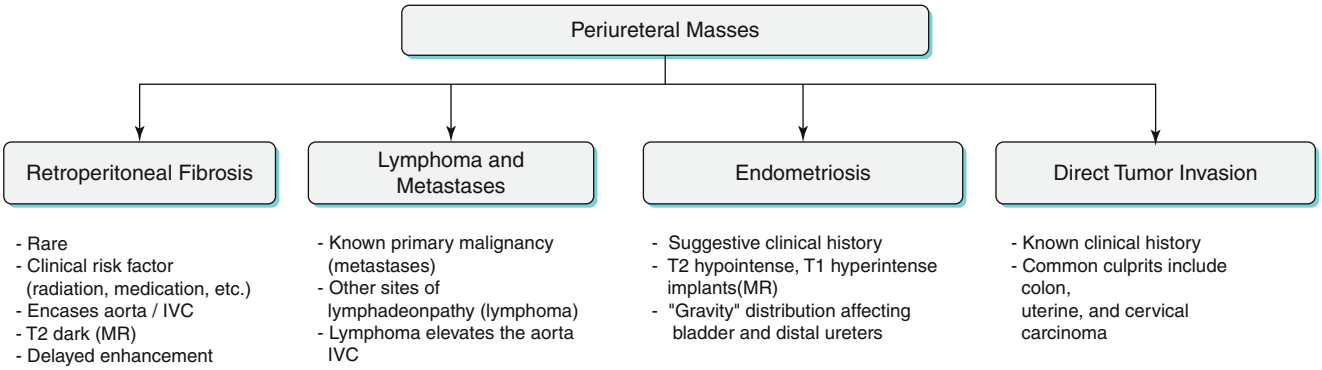

Algorithm 21.3 Common causes of periureteral masses and their imaging findings

lymphoma is rarely difficult, given the vast majority present as bulky, lobulated, sometimes confluent nodal masses. In cases where retroperitoneal fibrosis and lymphoma are both considered, helpful clues to a diagnosis of lymphoma include the following: any non-retroperitoneal site of nodal disease (mesentery, spleen, chest, pelvis, etc.), ureteral *displacement* rather than *retraction/stenosis*, and elevation of the aorta and IVC off the spine.

It is important to note that not all bulky retroperitoneal lymphadenopathy equals lymphoma, and metastatic disease must also be considered. Consideration of a primary malignancy is largely directed by known history and epidemiologic risk factors. In young adult men with periureteral or perirenal lymphadenopathy, a primary testicular malignancy (seminoma in particular) must be excluded. In middle-aged and older women, ovarian metastases may produce similar lymphadenopathy. In both cases, lymphatic spread along the gonadal vein may produce marked periureteral lymphadenopathy due to the close proximity between the gonadal vein and ureter.

Endometriosis

Endometriosis describes the ectopic implantation of functional endometrial glands and stroma outside the uterine cavity. The exact pathophysiology is controversial, but the most widely accepted theory is that of *retrograde menstruation*, whereby endometrial tissue essentially metastasizes through the fallopian tube to later deposit on the serosal surfaces of the abdominal and pelvic viscera [19]. Urinary tract involvement by endometriosis occurs in approximately 1–6 % of affected women [20]. Of these patients, the bladder is eight times more commonly involved than the ureter [20], with the distal ureter being the most commonly involved ureteral segment. Endometrial implants may progressively invade through the serosa and deeper tissue layers of the ureter, producing luminal narrowing and eventual obstruction [19].

The symptomatology of cyclical pelvic pain related to menstruation is usually sufficient for a clinical diagnosis of endometriosis, and laparoscopy remains the mainstay of both diagnosis and treatment. However, magnetic resonance imaging is gaining acceptance in preoperative staging of endometriosis and also detection of unusual or distant disease, including identification of urinary tract complications. On MRI, endometriotic implants in the pelvis demonstrate signal features similar to ovarian endometriomas. Endometriosis tends to demonstrate low T2 signal like that of fibrosis, yet intrinsic foci of high T1 signal (reflecting blood products) which are most suggestive to the diagnosis. Variable levels of mild to strong enhancement with gadolinium may be found.

Various patterns of ureteric dilatation and abnormal contour can occur secondary to specific pathologies. These patterns are described in Algorithm 21.4.

UVJ Obstruction

Like any site along the urinary tract, the most common cause of obstruction at the ureterovesicle junction (UVJ) is an impacted stone migrated from the kidney. Primary urothelial carcinoma of the bladder trigone can spread directly to obstruct the UVJ as well. Other intrinsic causes for UVJ obstruction are the same as those outlined above.

Primary Megaureter

Any obstruction at the level of the ureterovesicle junction (UVJ) may result in diffuse dilatation of the upper urinary tract

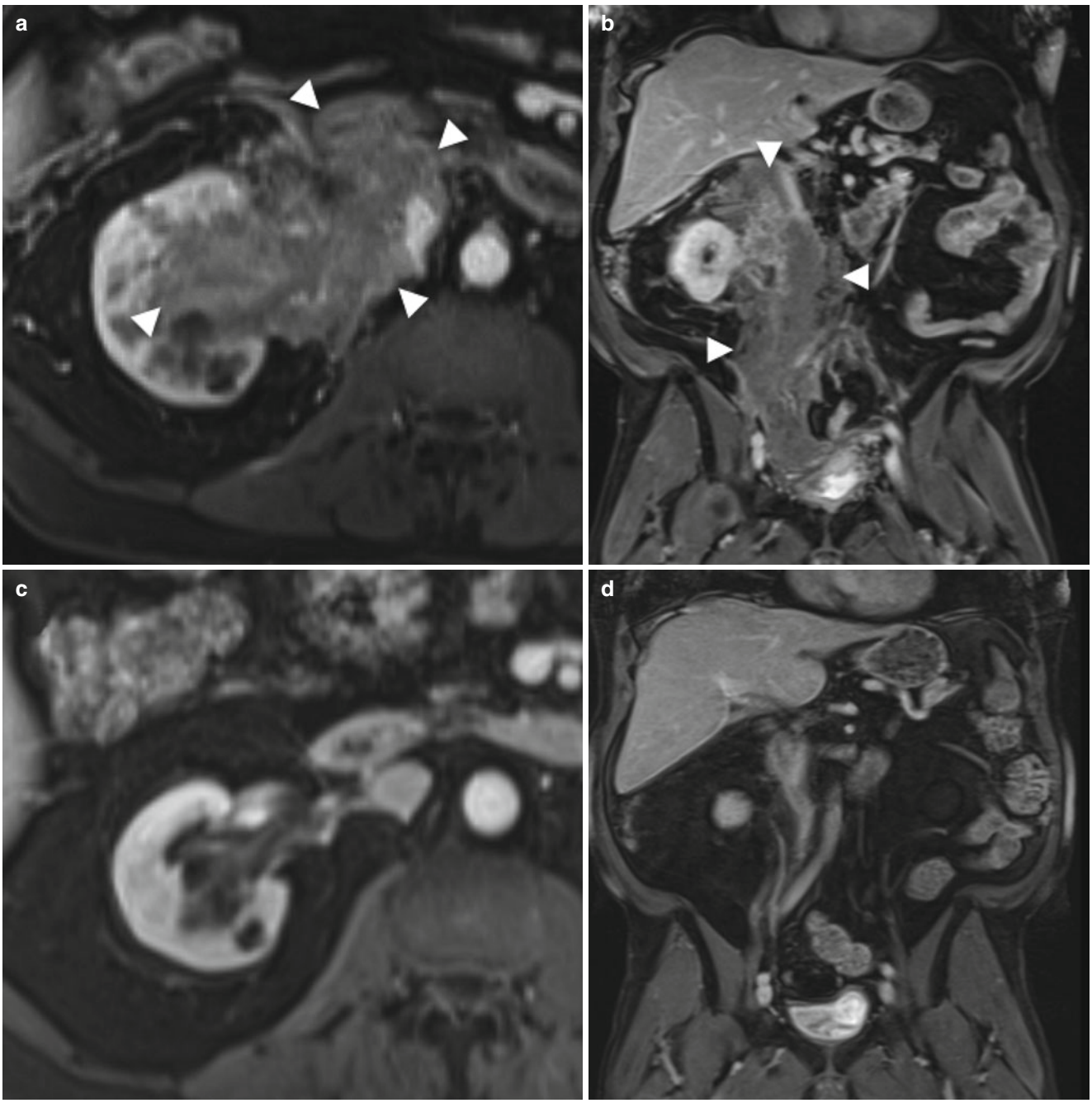

Fig. 21.15 Periureteral masses: Lymphoma/myeloma. Axial and coronal T1+Gd MR. (**a**, **b**) August 2011. Extensive enhancing soft tissue mass encasing entire length of the right ureter and renal pelvis, infiltrating the kidney. Histology revealed plasma cell dyscrasia consistent with multiple myeloma (demarcated by *arrowheads*). (**c**, **d**) October 2011. Dramatic improvement following chemotherapy

(Fig. 21.16). By far, the most common cause is a stone lodged at the ureterovesicle junction, followed by other acquired etiologies for obstruction: intrinsic bladder or ureteral tumor, extrinsic tumor invasion/encasement, as well as reactive changes seen with infection, inflammation, or pelvic irradiation.

On the other hand, congenital abnormality of the extreme distal ureteral segment, as in the case of *primary megaureter*, may mimic mechanical UVJ obstruction. Analogous to Hirschsprung disease of the colon, there is aperistalsis of a very short (0.5–4 cm) segment of distal ureter, just above the

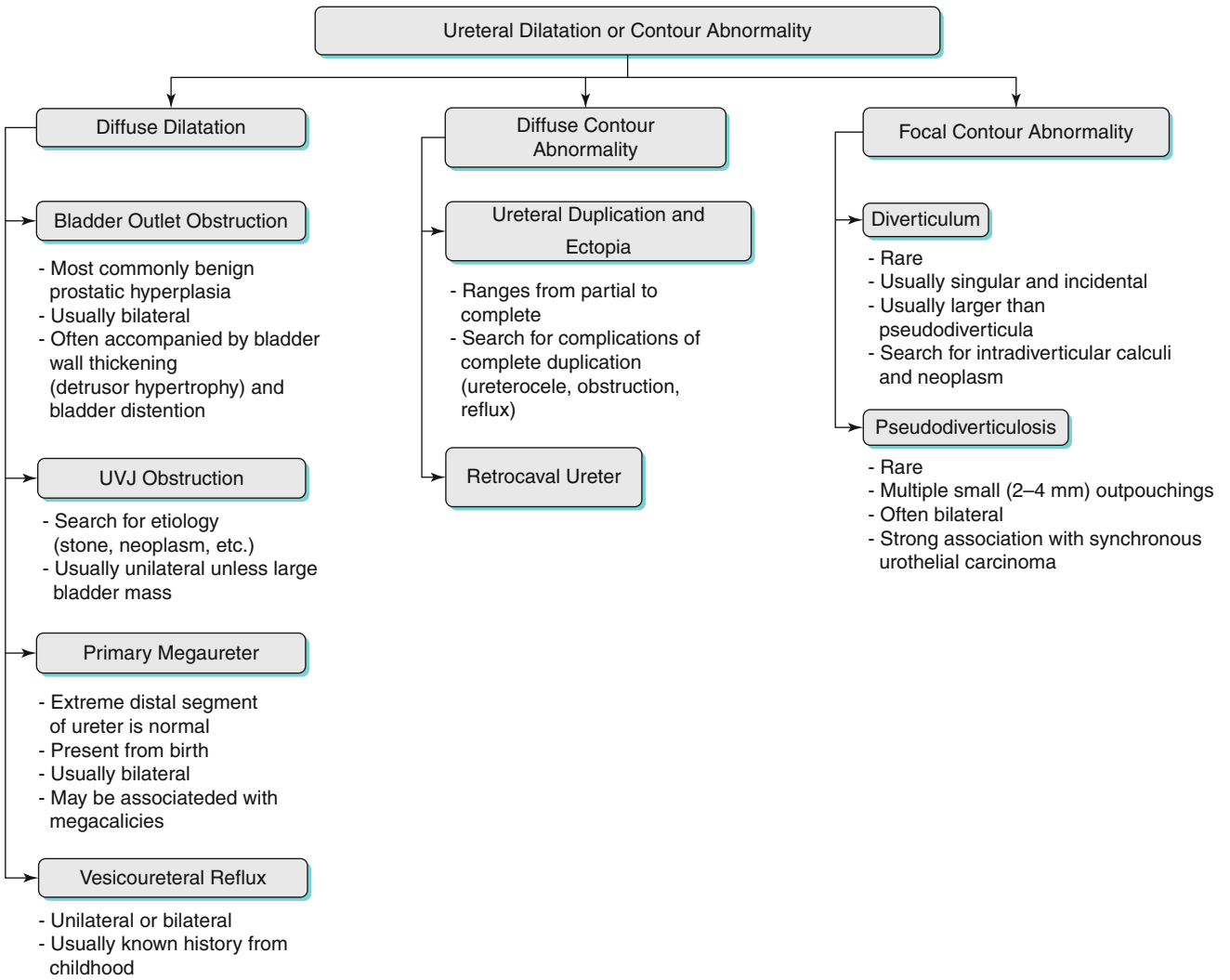

Algorithm 21.4 Systematic approach toward the evaluation of ureteral size or contour abnormalities

UVJ, with diffuse—often severe—dilatation of the upper urinary tract [21].

Vesicoureteral Reflux

Vesicoureteral reflux (VUR), as its name implies, defines the abnormal retrograde movement of urine from the urinary bladder into the ureter(s). This is mostly a problem encountered in young children and is attributed to a congenital abnormality of the ureterovesicle junction in which the tunneled segment of the distal ureter in the bladder wall is too short. With bladder distention, the UVJ is incompetent, allowing reflux of urine. VUR may also be seen in young boys with urinary obstruction from posterior urethral valves and in association with neurogenic bladder. In adults, acquired VUR may be seen in postsurgical cases where ureteral reimplantation has been performed.

The imaging mainstay in diagnosis of VUR in children is the voiding cystourethrogram (VCUG), during which reflux is observed during real-time fluoroscopy. VUR may be suspected at CT or MR when diffuse ureteral dilatation is present in the setting of bladder distention, especially when bilateral. In contrast to obstructive etiologies of diffuse ureteral dilatation, there is no stone or mass found at the UVJ. In contrast to primary megaureter, the entire distal ureteral segment is dilated, including the tunneled segment of the UVJ.

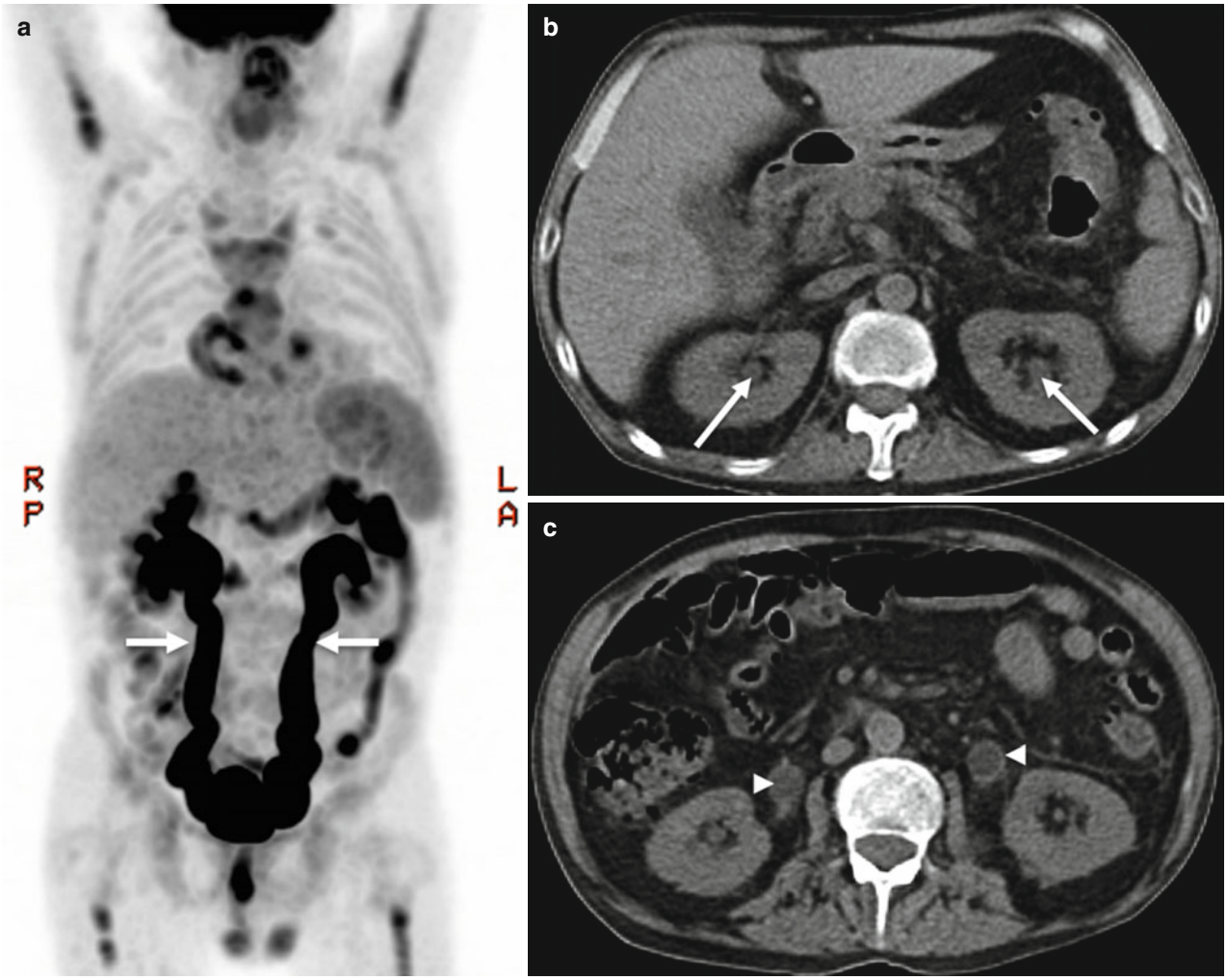

Fig. 21.16 Probable primary megaureter. (**a**) Whole body FDG-PET. Massive bilateral hydroureteronephrosis (*arrows*). (**b**, **c**) Axial NECT. Note marked bilateral ureterectasis (*arrowheads*) yet nondistended calyces (*arrows*)

Ureteral Diverticula and Pseudodiverticula

Compared to diverticula of the urinary bladder and renal calyces, diverticula of the ureter are rare. Congenital ureteral diverticula tend to be solitary and are often large outpouchings which are entirely incidental and asymptomatic, unless complicated by intradiverticular stone formation or infection (Fig. 21.17). Ureteral diverticula may also be acquired from prior stone disease, obstruction, infection, or instrumentation.

Ureteral pseudodiverticulosis (UPD) is a very rare entity with fewer than 80 cases reported in the literature between 1957 and 1991 [22]. Histologically, UPD are neither true nor false diverticula, instead made up of hyperplastic urothelium protruding into the loose subepithelial layers, forming crypts [23]. UPD is characterized by multiple small (<4 mm) ureteral outpouchings, bilateral in 70 % of cases, usually involving the proximal and midureteral segments [23]. UPD is found in association with chronic inflammatory changes and a striking incidence of synchronous urothelial carcinoma is reported, perhaps as high as 50 % [22].

Ureteral Duplication and Ectopia

Ureteral duplication is the most common congenital anomaly of the urinary tract, occurring in approximately 1 % of the population. Embryologically, the ureteral tube is formed during the cranial ascent of the *ureteric bud*. The ureteric bud then terminally branches to form the renal collecting system before finally inducing development of the kidney around it. Therefore, any premature branching of the ureteric bud can produce any degree of partial to complete ureteral

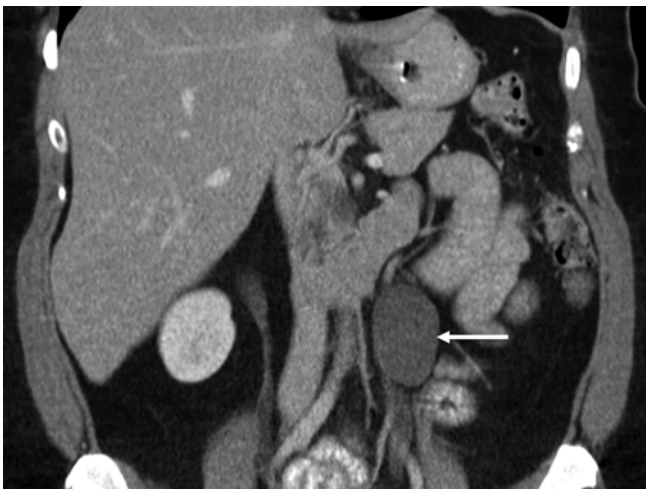

Fig. 21.17 Ureteral diverticulum. Coronal nephrographic phase CECT. Ovoid simple fluid attenuation structure contiguous with the left ureter consistent with a ureteral diverticulum (*arrow*)

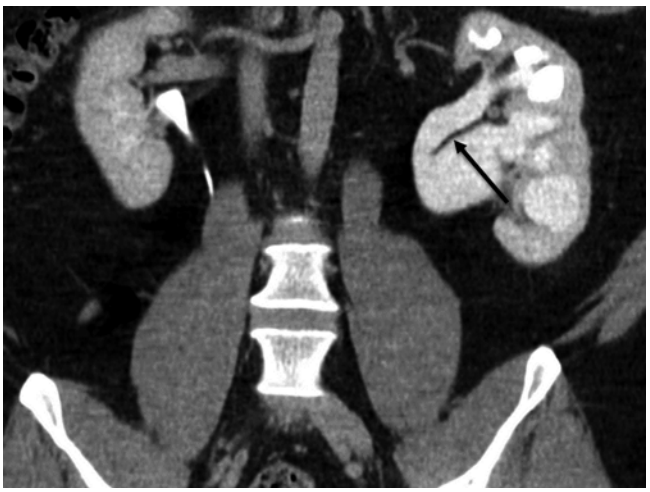

Fig. 21.18 Bifid renal pelvis. Coronal excretory phase CT urogram. Distinct cleft (*arrow*) dividing the left renal pelvis into two moieties, representing the mildest form of partial ureteral duplication. Incidental left UPJ obstruction

duplication. In most cases of ureteral duplication, the kidney also assumes a "duplex" appearance in which upper and lower pole moities are divided by a bridge of normal cortical tissue [24].

At the mildest end of the spectrum is a *bifid renal pelvis* (Fig. 21.18), in which there is separation of the renal pelvis into an upper moiety receiving the upper pole calyces and a lower moiety receiving the lower pole calyces. Both moieties converge at or above the ureteropelvic junction. As an isolated finding, a bifid renal pelvis is purely incidental and requires no clinical or imaging follow-up.

At the opposite end of the spectrum, there may be *complete duplication* in which two complete and separate ureters drain a single kidney (Fig. 21.19). The aberrant anatomy in this case generally follows the Weigert-Meyer rule, which states: *The lower pole ureter inserts at a normal (orthotopic) position in the posterior bladder wall. The upper pole ureter inserts ectopically, inferior and medial to the normal ureterovesicle junction.*

Complete ureteral duplication carries significant clinical implications. First, the ectopic ureter may protrude abnormally into the bladder lumen, producing an *ureterocele*, resulting in obstruction of the ureter and corresponding upper pole collecting system. Secondarily, the ureterocele can have mass effect on the adjacent orthotopic ureteral orifice, resulting in reflux to the lower pole moiety. Additionally, the ectopic ureter commonly inserts completely below the bladder neck and urogenital diaphragm (Figs. 21.20 and 21.21). In girls, insertion into the urethra or vagina causes recurrent infections and constant urinary dribbling. In boys, continence is maintained by the external urethral sphincter which lies at the base of the prostate.

In the middle of the spectrum is any degree of *partial ureteral duplication* in which a duplex kidney drains into two separate renal pelves with continuation as two separate ureters (Fig. 21.22). The two ureters may then unite at any level in the abdomen or pelvis, becoming a normal distal ureter which inserts normally (orthotopically) at the urinary bladder. Partial ureteral duplication is usually clinically insignificant, except for surgical implications such as donor nephrectomy and other genitourinary interventions.

Retrocaval Ureter

Aside from ureteral duplication, congenital anomalies of the ureter are extremely rare. Retrocaval ureter describes an anomalous course of the right ureter which deviates medially and passes behind the inferior vena cava, thus partially encircling it during the ureter's caudal path into the pelvis. If sufficiently compressed between the IVC and right psoas muscle, focal obstruction will occur leading to hydronephrosis (Fig. 21.23). Retrocaval ureter has an estimated incidence of 1 in 1,000 with a two- to threefold male predominance [25].

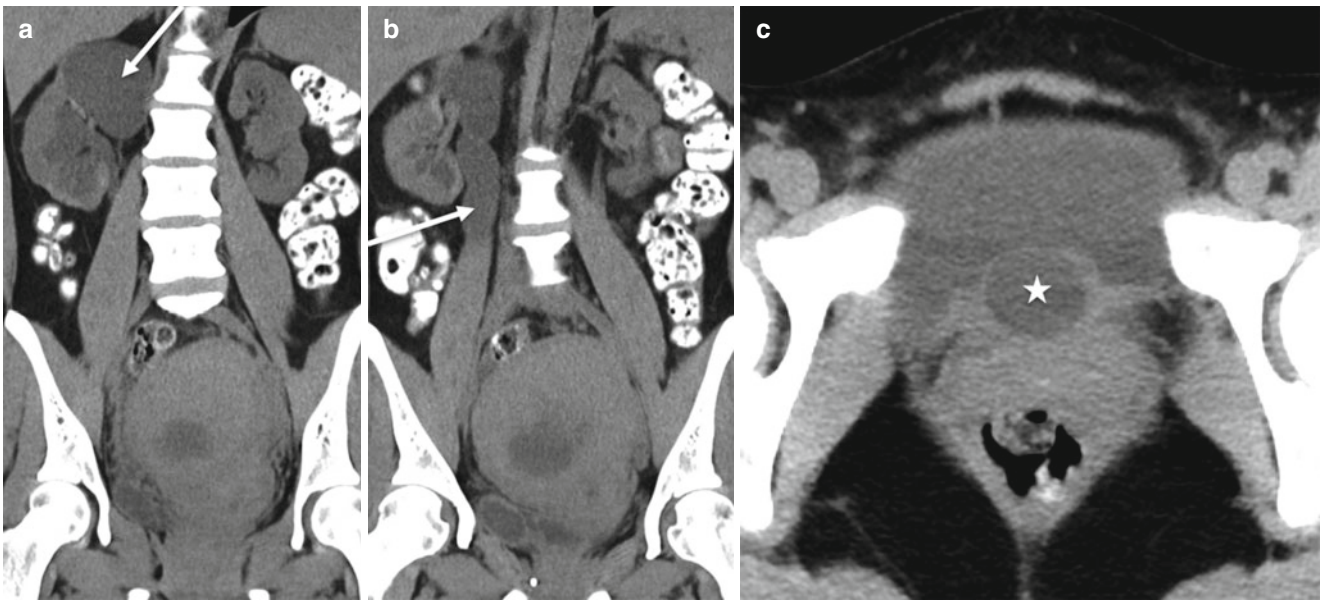

Fig. 21.19 Complete ureteral duplication. Noncontrast axial and coronal CT. (**a**, **b**) Markedly dilated collecting system and ureter of the upper pole moiety consistent with obstruction (*arrows*). Mildly dilated collecting system of the lower pole moiety likely secondary to reflux. (**c**) Thin-walled urine density sac within the posterior bladder found to represent ectopic ureterocele of the upper pole ureter (*star*)

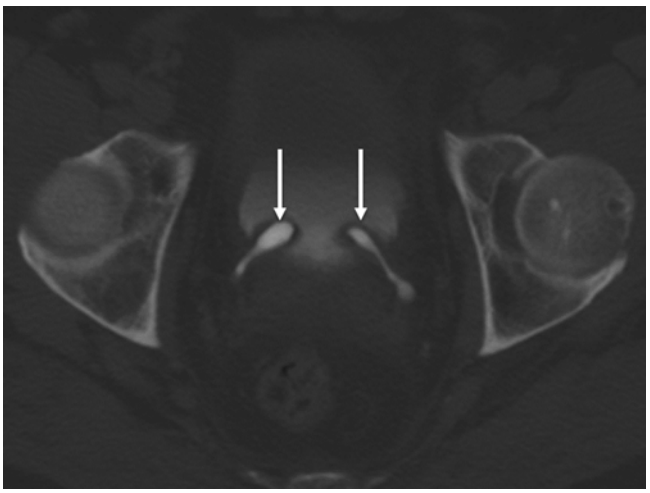

Fig. 21.20 Bilateral ureteroceles. Excretory phase CT urogram. Contrast-opacified structures protruding into the bladder lumen at the level of the ureterovesicle junctions consistent with simple ureteroceles (*arrows*)

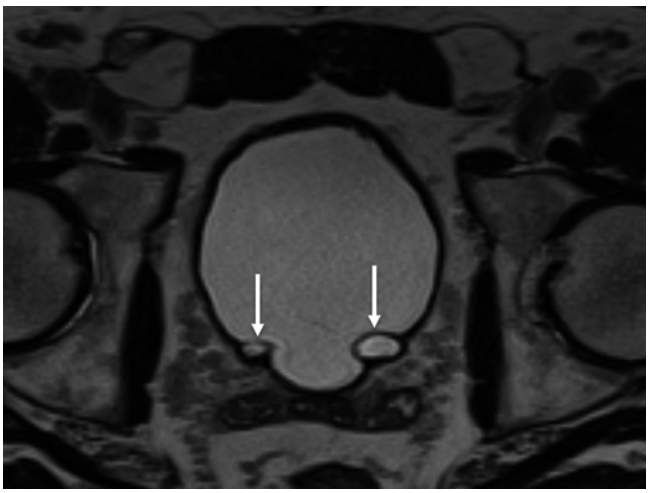

Fig. 21.21 Bilateral ureteroceles. T2-weighted axial MR. Thin-walled, fluid-signal structures protruding into the bladder lumen at the level of the ureterovesicle junctions consistent with simple ureteroceles (*arrows*)

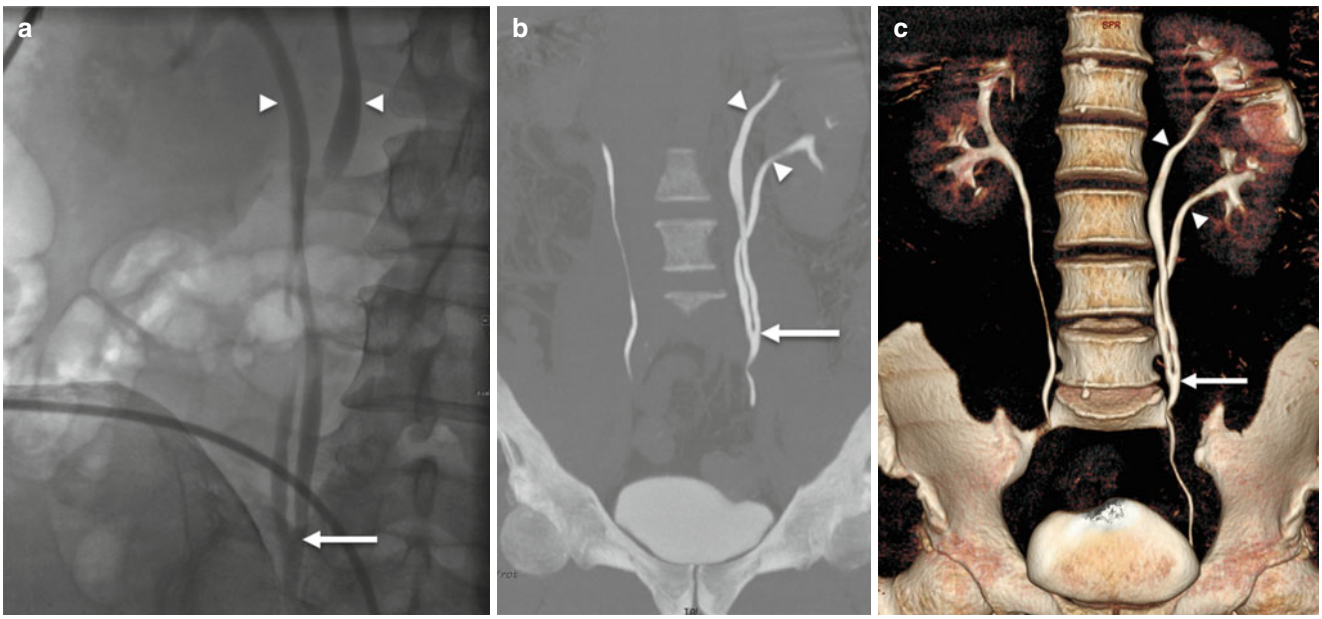

Fig. 21.22 Partial ureteral duplication. Antegrade pyelogram (posterior projection) (**a**); excretory phase CT urogram (**b**), coronal MIP and shaded surface 3D volume rendering (**c**). Duplicated left ureter (*arrowheads*) with upper and lower pole moieties joining (*arrows*) at the pelvic inlet

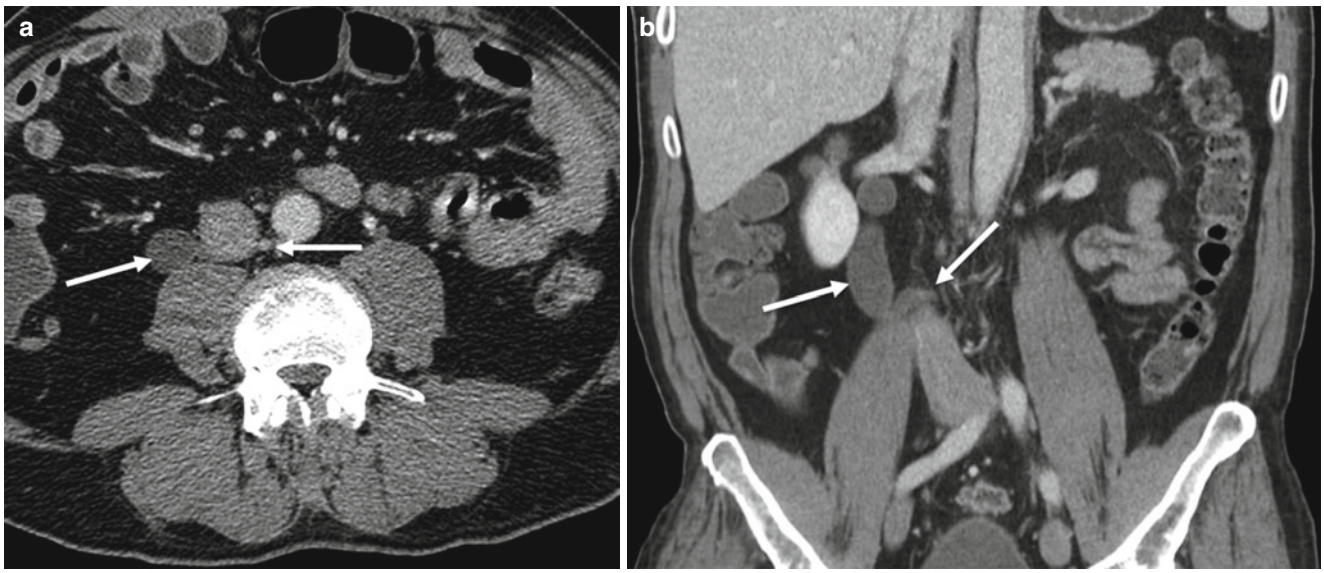

Fig. 21.23 Retrocaval ureter. Axial and coronal CECT. (**a**) Abrupt caliber change of the right ureter where it anomalously crosses behind the IVC (*arrows*). (**b**) Dilated right ureter proximal to an abrupt hook-like turn behind the IVC (*arrows*)

Upper Urinary Tract Infection

A more extensive discussion of urinary tract infection can be found later in the bladder section of this chapter. Since most upper urinary tract infection spreads retrograde from the urethra and bladder, infection of the ureter (*ureteritis)* and renal pelvis (*pyelitis*) is usually preceded by cystitis.

Imaging findings of ureteritis and pyelitis mirror those of cystitis. First, there is urothelial inflammation leading to diffuse thickening of the wall of the ureter or renal pelvis with surrounding fat stranding (Fig. 21.24). On post-contrast imaging, one might also see abnormal urothelial enhancement.

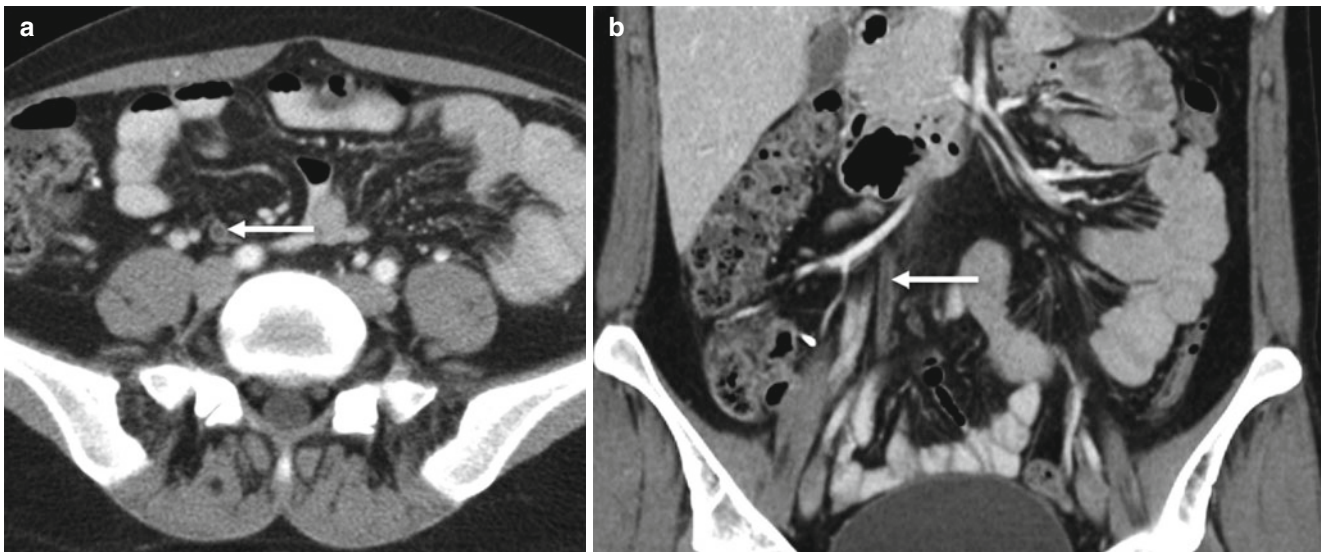

Fig. 21.24 Urothelial inflammation. Axial (**a**) and coronal (**b**) portal venous phase CECT. Abnormal thickening and enhancement of the right ureteral epithelium (*arrows*) with subtle periureteral fat stranding

Urinary Bladder

Normal Anatomy

The urinary bladder is the musculomembranous sac that serves as a reservoir for urine excreted by the kidneys, received from the ureters, prior to elimination from the body. Seated on the floor of the pelvic cavity, the peritoneal covering drapes over the bladder, covering only its superior and lateral surfaces. Internally, the bladder has three normal orifices: two opposite ureteral inlets along the posterior wall and the urethral orifice (bladder neck) at its base. The smooth triangular surface connecting these three points is named the *bladder trigone*, which is an important site for both harboring infection and development of urothelial carcinoma.

The bladder wall is composed of four layers, from external to internal: serosa, muscularis, submucosa, and mucosa. The serosa is partially derived from peritoneum. The muscular layer comprises three layers of smooth muscle which together form the detrusor muscle. The submucosa is a layer of connective tissue also known as the lamina propria, principally functioning to bind the mucosa to the more substantial muscular layer.

Finally, the internal lining of the bladder is the mucosa, a pliable epithelial layer termed *urothelium* (previously "transitional epithelium"), which can accordion into rugae when the bladder is contracted and stretch taut when the bladder is distended. The cells were originally termed *transitional* for their ability to transition from cuboidal cells in the nondistended bladder to flattened cells when the bladder is full.

Bladder Wall Thickening

Perhaps the most common of all bladder abnormalities identified on routine imaging is thickening of the bladder wall. After deciding that bladder wall thickness is present, the next decision point is determining whether thickening is focal or diffuse.

Urinary bladder wall thickening can be caused by various diseases. Algorithms 21.5 and 21.6 illustrate the spectrum of causes of urinary bladder wall thickening and their pertinent pattern.

Nondistention

Intuitively, the bladder wall thins as it stretches to the distended state, so any determination of bladder wall thickness must account for the degree of distention. Hakenburg et al. report the normal values for bladder wall thickness (BWT) as 3.0 ± 1 mm in normal adult women and 3.3 ± 1.1 mm in normal adult men [26]. In general, if the bladder is at least half full, the wall should measure less than 3 mm thick, although a visual assessment is often satisfactory. High resolution CT and MR easily allow visual assessment, as well as quantitative measurement. In the contracted state, diagnosis of bladder wall thickening should be made with caution, unless clinical history or secondary imaging findings are present.

Hypertrophy

Diffuse bladder wall thickening is commonly encountered in patients with chronic bladder outlet obstruction. This is a common scenario in men with benign prostatic hypertrophy. The detrusor muscle undergoes compensatory hypertrophy to facilitate voiding through the narrowed prostatic urethra,

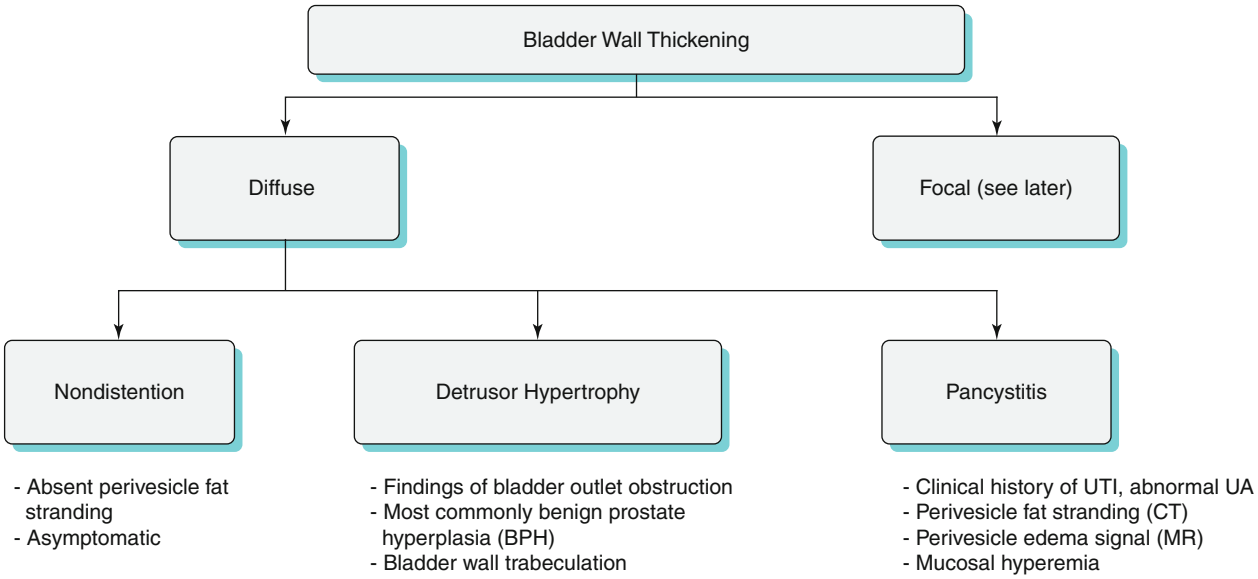

Algorithm 21.5 Causes of focal or diffuse bladder wall thickening

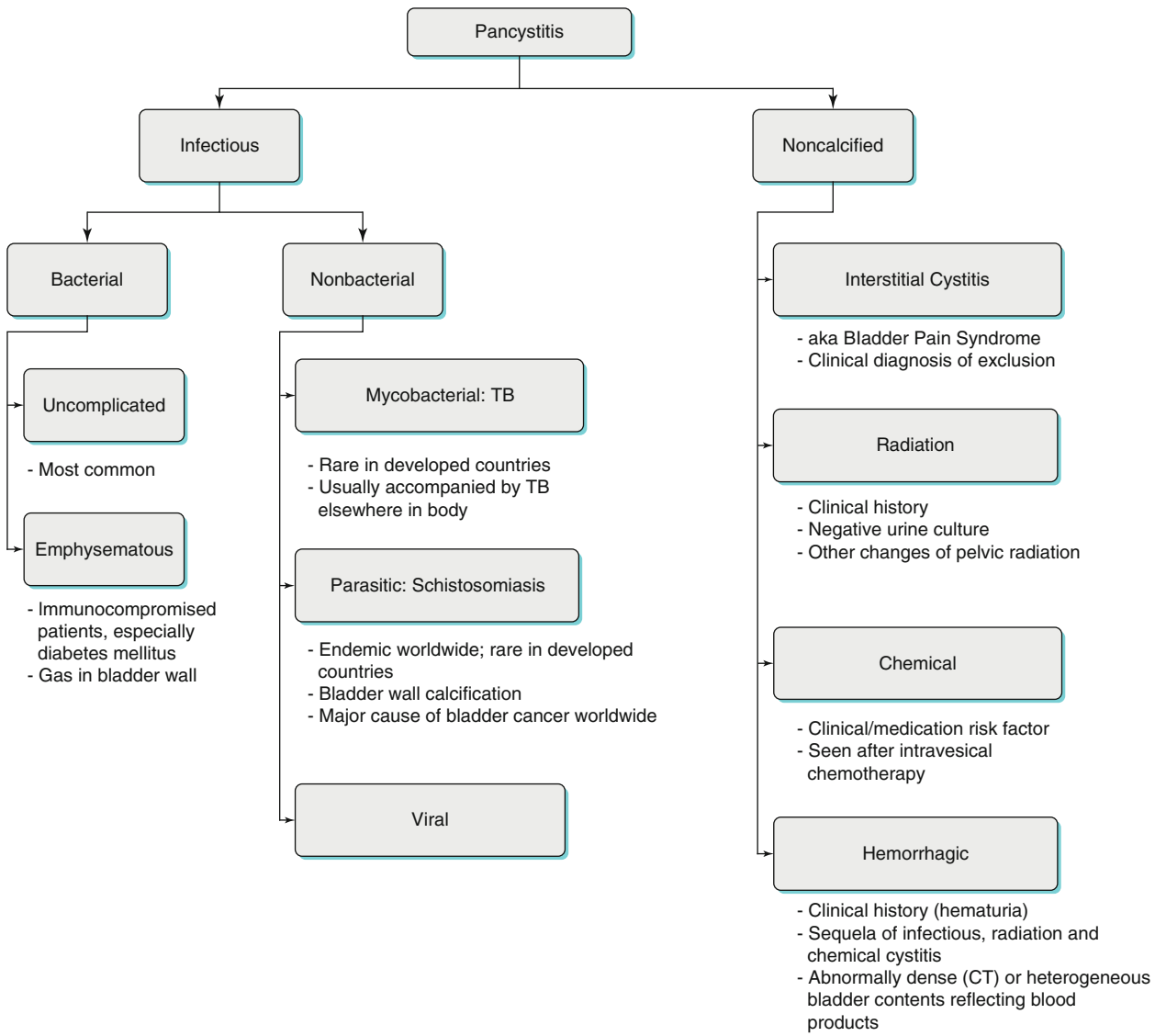

Algorithm 21.6 Etiologies of pancystitis

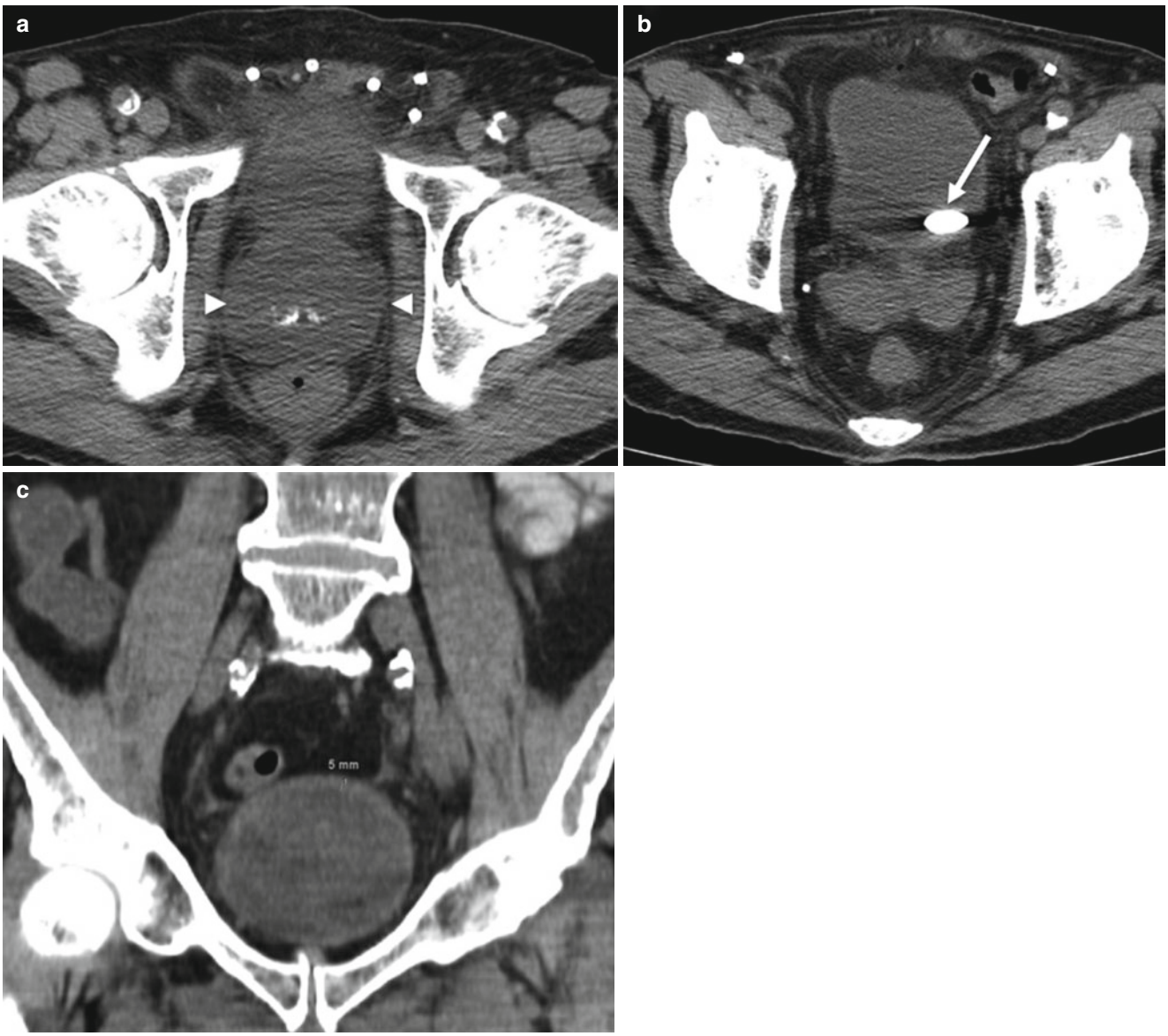

Fig. 21.25 Bladder outlet obstruction. (**a**) Axial noncontrast CT. Markedly enlarged prostate (*arrowheads* demarcate the transverse extent of the prostate) with central calcifications. (**b**) Ovoid hyperdensity lying dependently in bladder lumen consistent with large calculus (*arrow*). (**c**) Coronal noncontrast CT. Diffuse bladder wall thickening consistent with detrusor hypertrophy

resulting in diffuse bladder wall thickening visible on CT and MR (Fig. 21.25). Other chronic urethral strictures, most of which are secondary to prior infection or trauma, may result in bladder wall hypertrophy. Trabeculation can be exquisitely demonstrated on MR with high resolution T2-weighted sequences. Another clue to bladder outlet obstruction is the presence of pulsion diverticula of the bladder wall, discussed later in this chapter.

Pancystitis

Cystitis refers to inflammation of the urinary bladder by any cause. Although cystitis encompasses many etiologies, the result of bladder irritation produces a similar clinical and radiologic picture. Often, there is a constellation of increased urinary frequency, dysuria (painful urination), suprapubic discomfort, and rarely hematuria. Hematuria, when present, is usually microscopic.

Uncomplicated cystitis is a clinical diagnosis and, in most cases, imaging is not required. However, imaging may be utilized to identify potential causes of unexplained or recurrent infection, to rule out secondary findings such as stones or hydronephrosis, and to evaluate complicated cases such as emphysematous cystitis. Imaging also has a wide role in problem solving when the clinical diagnosis is unclear or when the patient does not respond to standard treatment. Besides clinical history and urinalysis, secondary imaging findings beyond bladder wall thickening include perivesicular inflammatory changes: fat stranding on CT, T2 hyperintense

edema signal on MR. With acute inflammation, hyperemia of the bladder mucosa is seen as a thin line of hyperenhancement along the inner surface of the bladder wall.

Uncomplicated Bacterial Cystitis

A majority of cystitis is acute bacterial cystitis, caused by retrograde infection through the urethra. Women are more frequently affected then men, because of the short length of the urethra and local perineal spread of bacteria from the vagina or anus. Hematologic dissemination of bacterial cystitis is also possible, particularly in immunocompromised individuals, resulting in urosepsis.

In children, and to a lesser extent in adults, cystitis in the acute phase is usually self-limited following adequate treatment. However, when infection spreads retrograde (as in a child with vesicoureteral reflux), then pyelonephritis may develop and, with it, the attendant risks of renal parenchymal scarring and loss of function. This explains the reason for aggressive screening for VUR in children with urinary tract infection.

Emphysematous Cystitis

Emphysematous cystitis is an uncommon complication of urinary tract infection in the adult, occurring most frequently in patients with poorly controlled diabetes mellitus. Additional risk factors include neurogenic bladder, chronic bladder infection, and other immunocompromised states besides diabetes [27]. As its name implies, emphysematous cystitis is characterized by gas in the urinary bladder wall, owing to bacterial fermentation of glucose and its gaseous by-products. It is most commonly the result of *Escherichia coli*, *Enterobacter aerogenes*, or *Clostridium perfringens* [27]. Unique among infectious bladder conditions, this entity can be diagnosed by radiography, in which a ring of gas bubbles project along the contour of the bladder wall. CT further increases sensitivity for emphysematous cystitis, allowing visibility of even small amount of gas in the bladder wall. On MRI, gas within the bladder produces dark signal voids on both T1- and T2-weighted sequences.

Nonbacterial Infectious Cystitis: TB, Schistosomiasis

Two forms of infectious cystitis deserve specific mention, mainly for their historical significance, at least in Western medicine: *tuberculosis and schistosomiasis.* These two entities, outside the developing world, are far more common in radiology case conferences than clinical practice.

Schistosomiasis

Schistosomiasis is a parasitic infestation of the urinary bladder caused by *Schistosoma haematobium*. Although very rare in developed nations, schistosomiasis remains an important cause of cystitis and bladder cancer worldwide. According to 2011 data from the World Health Organization, an estimated 207 million people are infected worldwide, and an estimated 700 million people are at risk for infection secondary to infested water sources [28]. After penetrating the skin, *S. haematobium* undergoes a complex life cycle in the human host before migrating to the bladder through the perivesicular venous plexus [28]. Once deposited in the bladder wall, a granulomatous inflammatory reaction ensues, leading to fibrosis and calcification. Schistosomiasis is the most common cause of bladder cancer worldwide [29].

Tuberculous Cystitis

Tuberculous cystitis is classically characterized by slow increase in thickening of the bladder wall and diminution of bladder volume. Tuberculosis (TB) of the bladder is usually accompanied by TB at other sites in the body, including pulmonary TB. Unique among urinary tract infection, tuberculosis almost always spreads *antegrade* from the kidney, down the ureter, to involve the bladder secondarily. Chronic TB of the bladder incites a granulomatous reaction and fibrosis of the bladder wall, leading to a low capacity bladder and bladder wall calcification, although calcifications are much less commonly seen with TB than with schistosomiasis.

Various diseases can lead a spectrum of focal and diffuse patterns of urinary bladder wall calcification. Familiarity with these patterns can help radiologists to make a practical differential diagnosis and reach a specific diagnosis. Algorithm 21.7 illustrates common etiologies for urinary bladder wall calcification and their pertinent pattern of involvement.

Noninfectious Cystitis: Interstitial Cystitis, Eosinophilic Cystitis, and Radiation and Chemotherapy

Interstitial Cystitis

Interstitial cystitis (IC), also known as *bladder pain syndrome (BPS),* is a chronic bladder inflammatory syndrome of unclear etiology or pathogenesis. Approximately 1 million patients in the United States are diagnosed with IC/BPS each year, with a significantly higher incidence of involvement (90 %) among women. Interstitial cystitis may attain an ulcerative or a non-ulcerative form. In the classic ulcerative form, Hunner's ulcers are typically present on the internal surface at the dome of a thickened urinary bladder, which is small and decreased in capacity. Histologically, IC is characterized by fibrosis of the deep layers of the bladder wall. Nevertheless, IC remains a clinical diagnosis of exclusion and indistinguishable from other causes of pancystitis. The role of imaging is to exclude other causes of pain if the urologist is considering the diagnosis of IC [30].

Eosinophilic Cystitis

Eosinophilic cystitis is a rare form of cystitis that may occur in children or adults. Eosinophilic cystitis is usually seen in

Algorithm 21.7 Etiologies of bladder wall calcification

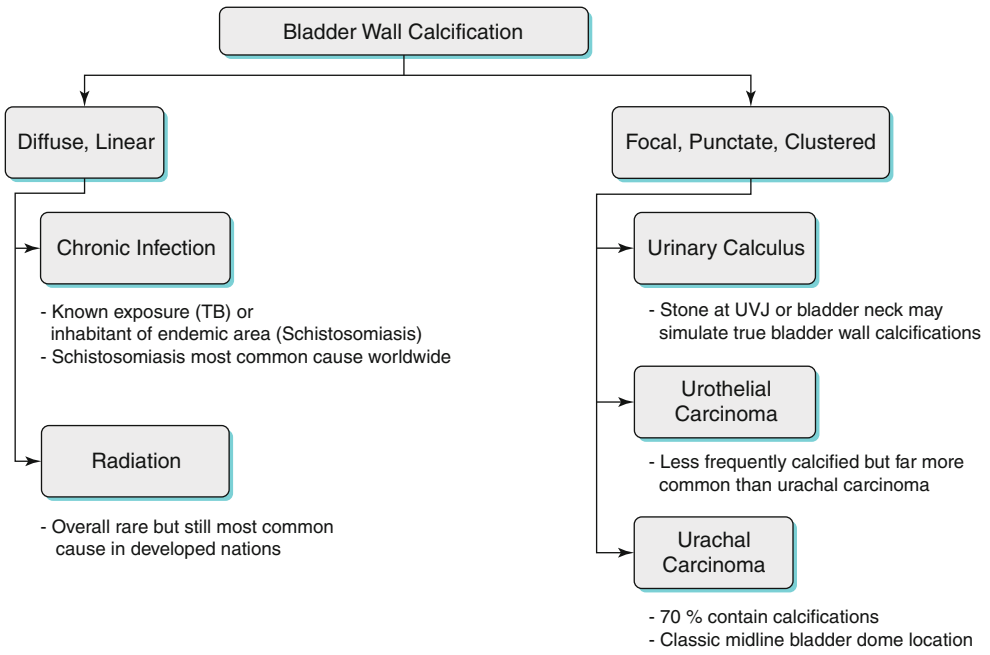

patients with atopic syndrome—those with asthma, eczema, food or pollen allergies, as well as eosinophilic gastroenteritis. Imaging findings are no different than uncomplicated bacterial cystitis, and this is a clinical diagnosis.

Radiation and Chemotherapy

Radiation- and chemotherapy-induced cystitis should be evident from the patient's history, but imaging can help determine the magnitude of anatomic alteration and attendant inflammation and exclude associated complications. Both radiation and chemotherapy may induce hemorrhagic cystitis, leading to complex appearance of urine within the bladder lumen. As expected, bloody urine measures greater than simple fluid attenuation on CT and demonstrates intrinsically elevated signal on T1-weighted MR images.

In the absence of known history, another possible clue to radiation cystitis may be a low bladder volume secondary to poor distensibility. Radiation changes may be seen in the pelvic bones and bowel loops, and thickening of the presacral soft tissues may be seen. Chronic sequelae of pelvic and bladder irradiation include adhesive tethering and fistula formation. Gas in the urinary bladder, in the absence of recent instrumentation or catheterization, is virtually diagnostic of a fistula.

Focal Bladder Wall Thickening and Filling Defects

Focal bladder wall thickening (BWT) is much less commonly encountered than diffuse wall thickening. Although occasionally caused by nonneoplastic conditions, focal bladder wall thickening should be considered neoplastic until proven otherwise. In many cases, cystoscopy and tissue sampling are necessary to exclude malignancy.

A filling defect in the urinary bladder refers to any interruption in the homogeneous urine normally filling the bladder lumen. The identification of focal BWT and filling defects depends on multiple factors. Imaging modality and technique play a major role. On noncontrast CT, only structures that differ sufficiently from the fluid attenuation of urine may be easily identified, and many lesions—including bladder neoplasms—may be very subtle or even indistinguishable. On routine postcontrast CT (portal venous phase), enhancing lesions gain conspicuity on the background of low density urine. Furthermore, contrast-enhanced delayed phase CT allows time for dense contrast material to opacify the urine and reach the bladder, thus outlining any filling defects and permitting detailed evaluation of their size and shape. Finally, MRI allows easy identification of most filling defects on the backdrop of T2 hyperintense urine.

Bladder Calculi

Bladder calculi are not uncommon, mostly representing calculi that have migrated from the upper urinary tract, but may also be arising de novo in the setting of urinary stasis. As such, bladder outlet obstruction is the most common cause of de novo bladder calculi. Alterations in chemical and mineral concentrations in the urine may also contribute to their formation. Bladder inflammation secondary to radiation or from chronic infection with schistosomiasis is also a known cause.

Bladder calculi are often discovered incidentally but may also be the culprit for symptoms of cystitis secondary to mechanical irritation of the bladder wall, as well as urinary obstruction. Bladder calculi can also harbor bacteria, poten-

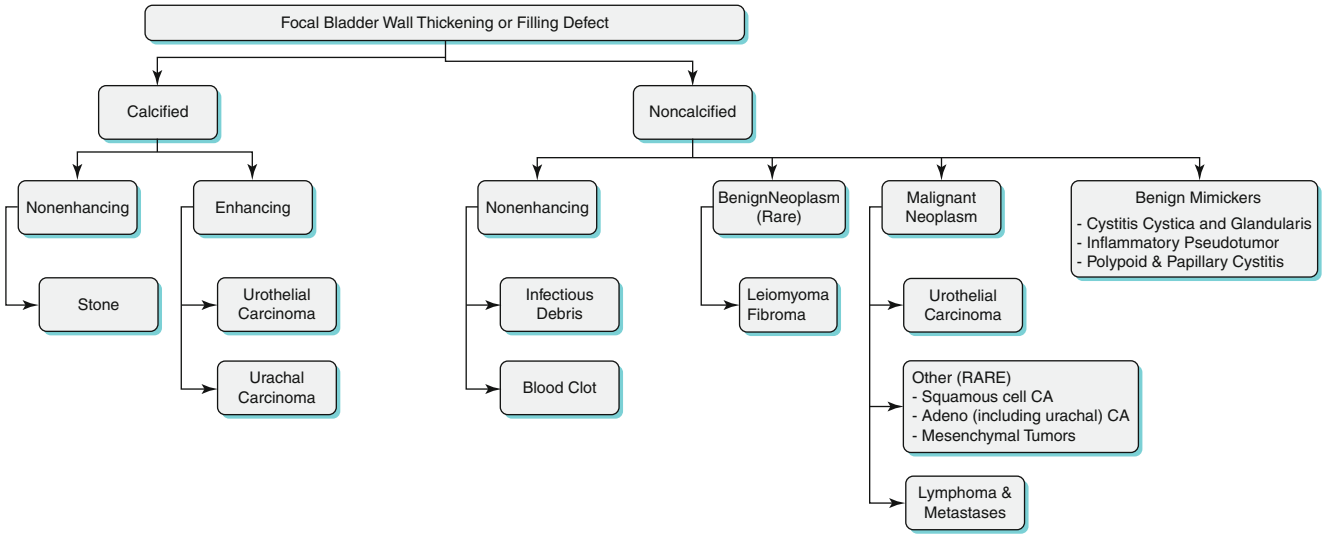

Algorithm 21.8 Systematic evaluation of focal calcified or noncalcified bladder wall thickening or bladder filling defect

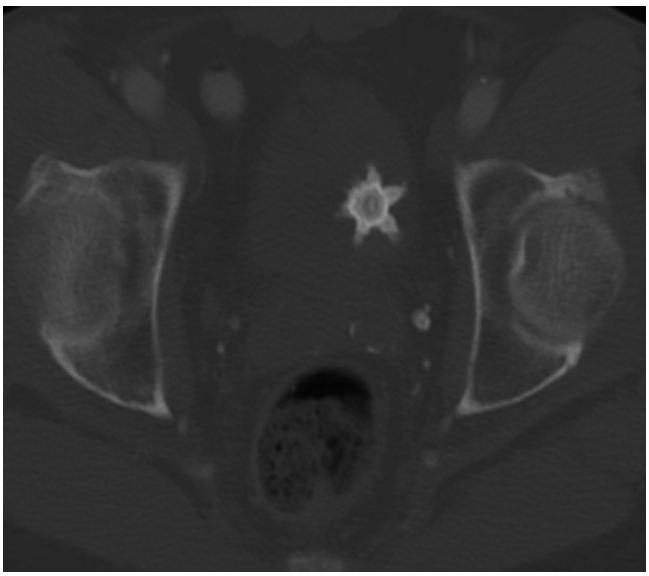

Fig. 21.26 Stellate bladder calculus. Axial noncontrast CT. Star-shaped hyperdensity in bladder lumen consistent with stellate calculus. Shape reflects its crystalline structure

tially leading to recurrent urinary tract infections (Fig. 21.26).

Bladder Cancer

Understanding the histology of the bladder wall is important, as bladder neoplasms can arise from any layer of the bladder wall. Bladder cancers are broadly classified as either epithelial or mesenchymal. As in the upper urinary tract, epithelial neoplasms account for the vast majority (95 %) of cases. Epithelial tumors are subdivided into urothelial carcinoma (i.e., transitional cell carcinoma), squamous cell carcinoma, and adenocarcinoma. Mesenchymal tumors are rare and include rhabdomyosarcoma (seen in children), leiomyosarcoma (seen in adults), as well as lymphoma, solitary fibrous tumor, and benign leiomyoma [31].

In the United States, bladder cancer is common, accounting for 2–6 % of all tumors and representing the fourth most common malignancy. Smoking is the most common preventable risk factor, but certain occupational exposures also have been implicated, especially industrial chemicals previously used to make certain dyes such as benzidine, aniline, and others. Male sex and advanced age are other risk factors [31].

Urothelial Carcinoma

Urothelial carcinoma (UC) is the current and preferred term for what is widely called *transitional cell carcinoma (TCC).* These represent the most common (90 %) of all bladder cancers and arise from the inner lining of the bladder, i.e., the "transitional" urothelium. According to American Cancer Society statistics, over 60,000 new cases of urothelial carcinoma were reported in 2005 [32]. Staging is determined by depth of invasion (determined histologically) and the presence of metastases, which is the primary role of imaging once the diagnosis is established [31].

When patients with bladder cancer return for restaging examinations, it is important to know what, if any, treatments have occurred. Superficial, polypoid urothelial carcinomas may be amenable to transurethral (cystoscopic) resection, which may result in focal bladder wall thickening early on secondary to edema and later from scar tissue and fibrosis (Figs. 21.27 and 21.28). MR may be helpful in these cases, as urothelial carcinoma is usually intermediate in T2 signal compared to the dark signal typical of fibrosis. Furthermore, urothelial carcinoma usually demonstrates earlier enhancement compared to the delayed enhancement typical of fibrosis. Nevertheless, periodic cystoscopy remains the gold standard to monitor for recurrent mucosal lesions, while

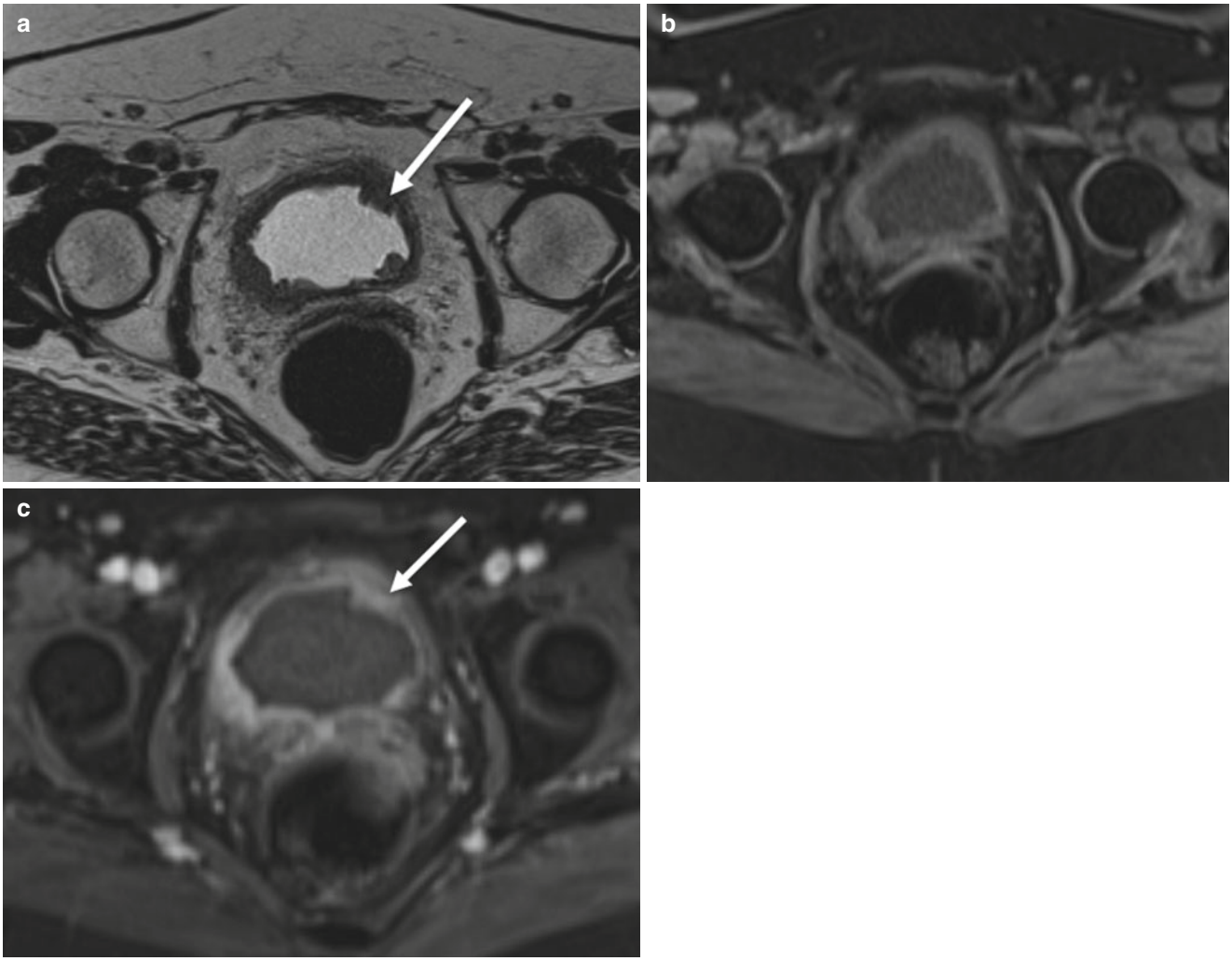

Fig. 21.27 Urothelial carcinoma. Axial T2 (**a**), T1 (**b**), and T1+Gd (**c**). (**a**) Irregular bladder wall thickening with intraluminal irregularity (*arrow*). (**b**) and (**c**) Plate-like enhancement of the bladder wall with focal enhancing polypoid projections (*arrow*). Multifocal urothelial carcinoma

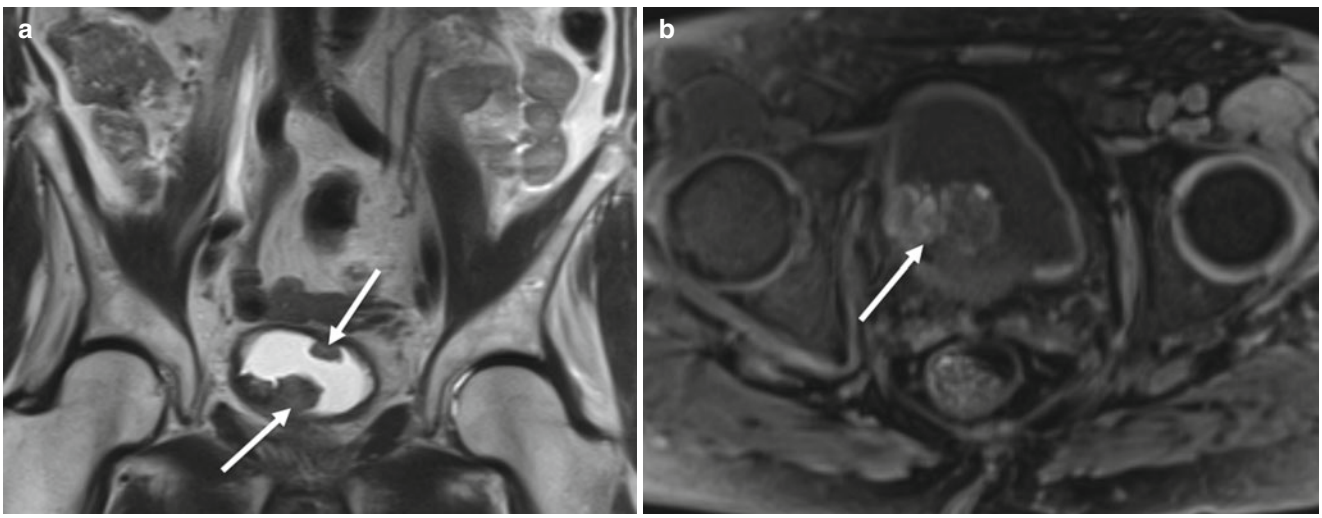

Fig. 21.28 Bladder urothelial carcinoma. (**a**) Coronal T2-weighted MR. Multiple polypoid mass growing from bladder wall, protruding into bladder lumen (*arrows*). (**b**) Axial T1+Gd. Heterogeneous weak enhancement (*arrows*)

imaging plays an important role to monitor for invasive and metastatic disease.

Many patients with bladder cancer also undergo intravesicular chemotherapy, which may result in diffuse bladder wall thickening and enhancement related to irritation. Patients with unresectable disease may undergo radiation and/or systemic chemotherapy for palliation, either of which may generate diffuse bladder wall thickening.

Squamous Cell Carcinoma

Although squamous cell carcinoma accounts for less than 5 % of bladder neoplasms in the United States, it supersedes urothelial carcinoma in parts of the world where schistosomiasis is endemic. In the United States, squamous cell carcinoma is seen in association with chronic inflammation in which there is squamous metaplasia of the normal urothelium and subsequent malignant transformation. The imaging appearance of squamous cell carcinoma is nonspecific; it occurs most often as a sessile growth or simply a region of focal wall thickening. It does not usually present as an isolated pedunculated mass like that characteristic for UC. Many of these patients have advanced local extension of disease at the time of diagnosis, with direct extravesical extension; however, metastases are relatively uncommon [33].

Adenocarcinoma (AC)

Adenocarcinoma of the bladder is subdivided into primary or secondary cancer, urachal or nonurachal. Most adenocarcinoma of the bladder is secondary (metastatic), while primary adenocarcinoma is rare and usually arises in a persistent urachal abnormality.

Mesenchymal Tumors

Mesenchymal bladder tumors are far less common and will be addressed briefly. Benign tumors include leiomymoma, paraganglioma, fibroma, hemangioma, and lipoma. Malignant tumors include rhabdomyosarcoma (seen mainly in children), leiomyosarcoma, lymphoma, and osteosarcoma [34].

Invasive/Metastatic Disease

Like anywhere in the body, the bladder may be a site of metastatic disease. The bladder may also be secondarily invaded by local pelvic malignancies, most often cervical and uterine carcinoma in women, prostate carcinoma in men, and colorectal carcinoma.

Benign Mimickers of Bladder Neoplasm

Polypoid and Papillary Cystitis

Polypoid and papillary cystitis is characterized by inflammation, vascular proliferation, and edema of the lamina propria. This is most commonly associated with long-standing catheterization [34]. Because of its mass-like appearance, it can easily be mistaken radiologically for tumor. Indeed, biopsy is often required to distinguish polypoid/papillary cystitis from urothelial carcinoma [34].

Cystitis Cystica and Cystitis Glandularis

Similarly, cystitis cystica and cystis glandularis (CCCG) have a well-known tendency to masquerade as bladder neoplasms, owing to their often mass-like and ominous appearance. It should be noted that small amounts of CCCG are often noted incidentally on biopsies done for other reasons [34].

Inflammatory Pseudotumor

Inflammatory pseudotumor is a rare lesion that occurs in virtually every organ of the body, including the urinary bladder. Inflammatory pseudotumor is mass like, measuring 2–8 cm, with a gel-like consistency at cystoscopy. Some experts refer to it as pseudosarcomatoid fibromyxoid tumor, as this describes its histologic findings of loosely packed spindle cells within a myxoid matrix. Although it may arise secondary to chronic irritation and inflammation, its etiology is unknown. It is not distinguishable from malignancy and can be locally aggressive. Fortunately, inflammatory pseudotumor does not metastasize and does not recur following resection [34].

Bladder Wall Contour Abnormality

Diverticula

A urinary bladder diverticulum is a weaknesses in the muscular bladder wall through which mucosal layers penetrate. The sac-like result does not function like the normal bladder wall due to its pedunculated morphology and loss of muscle-assisted motion. As such, diverticula are regions of urinary stasis.

Congenital diverticula are referred to as Hutch diverticula, are typically solitary, and are characteristically located superior and lateral to the ureteral orifice. Hutch diverticula are more common in males and are thought to be secondary to congenital localized weakness in the detrusor muscle.

Far more common are *acquired diverticula*, developing in response to elevated bladder pressure. Acquired diverticula are commonly seen in cases of neurogenic bladder or when the bladder outlet is obstructed from prostatic hypertrophy (Fig. 21.29). Prior trauma, including iatrogenic trauma, are other causes. Acquired bladder diverticula can occur in any location, are usually multiple, and are often seen in association with generalized trabeculation of the bladder wall.

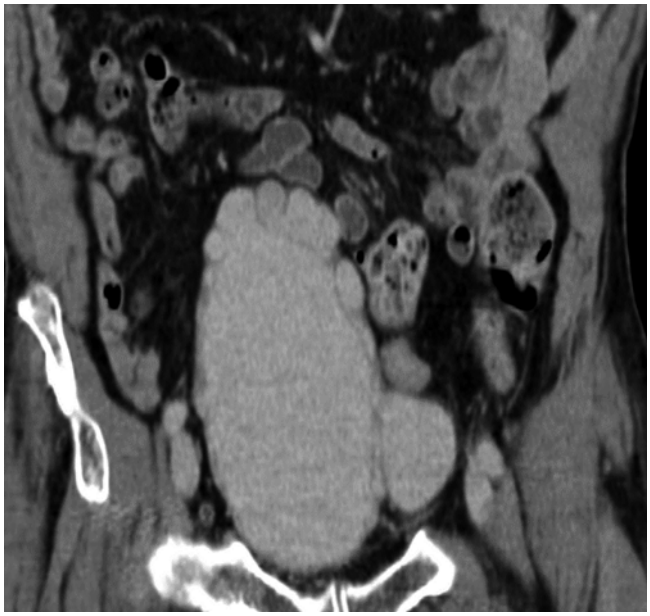

Fig. 21.29 Bladder diverticulosis. Coronal excretory phase CT urogram. Numerous contrast-filled outpouchings of the bladder wall consistent with diverticula. Patient suffered from chronic bladder outlet obstruction related to benign prostatic hyperplasia (BPH)

Like anywhere in the urinary tract, urinary stasis within a bladder diverticulum may lead to stone formation, infection, and inflammation. Furthermore, chronic inflammation may lead to urothelial squamous metaplasia and subsequent malignant transformation into squamous carcinoma (Fig. 21.30). Overall, the incidence of intradiverticular bladder carcinoma is 1–10 % [35]. Since diverticula inherently penetrate the muscularis tissue layer, carcinoma within a bladder diverticulum has a thinner boundary for extravesicular spread and, therefore, carries a worse prognosis than non-diverticular bladder carcinoma. Any finding of soft tissue within a urinary bladder diverticulum should be treated as cancer until proven otherwise. Early diagnosis is key, and a high index of suspicion is paramount.

Urachal Remnants

During embryologic development, the urinary bladder begins at the level of the umbilicus before gradually descending into the pelvis. Along the path of descent, a tubular sinus known as the *urachus* forms, through which urine empties in early development. Normally, the urachus undergoes fibrous involution by the third trimester, replaced by a microscopic fibrous strand, the median umbilical ligament. Therefore, any failed closure of the fluid-filled urachus will result in a spectrum of *urachal remnants* [36].

A *patent urachus* reflects 50 % of congenital urachal anomalies and should present early with urinary leakage from the umbilicus. In adults, urachal remnants are usually incidental findings, most commonly the *urachal cyst*, an isolated midline simple cyst between the umbilicus and bladder dome. *Urachal sinus* is less common, occurring as a blind sac at the umbilicus, and may be complicated by infection. Finally, the *urachal diverticulum* is often noted as a midline protrusion of the bladder dome. Not all urachal diverticula are congenital. In the case of chronic bladder outlet obstruction, an *acquired* urachal diverticulum may form, just as other acquired diverticula form at points of anatomic weakness.

Although usually incidental, urachal remnants are important to identify and to exclude any complication by infection or neoplasm. Although urachal carcinoma is rare, accounting for only 0.5 % of all bladder cancer [36], urachal carcinoma carries a poor prognosis. Since many lesions are clinically silent due to their location, disease is often either locally invasive or metastatic at presentation. In contrast to bladder cancer (urothelial carcinoma), a majority of urachal cancer is mucin-producing adenocarcinoma. Most urachal carcinomas arise at or near the bladder dome, thus they are easily confused with—or indistinguishable from—apical bladder carcinoma. However, the presence of calcification within such a mass is highly suggestive of a mucinous urachal carcinoma, rather than typical urothelial carcinoma.

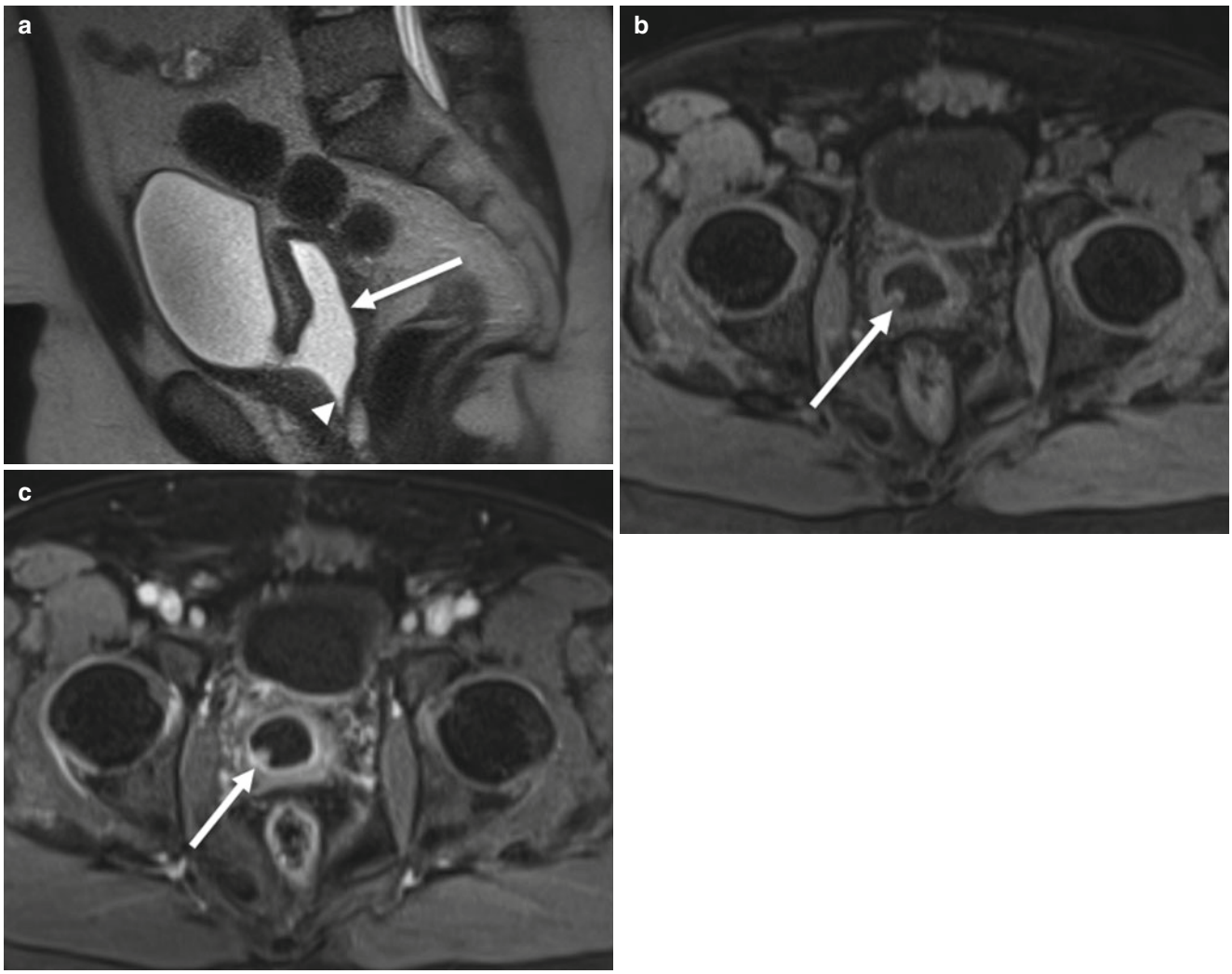

Fig. 21.30 Intradiverticular carcinoma. Sagittal T2 (**a**), axial T1 (**b**) and T1+Gd (**c**). (**a**) Large, thick-walled posterior bladder diverticulum (*white arrow*) associated with postsurgical changes of prior TURP (*white arrowheads*). (**b**, **c**) Enhancing nodule, right posterolateral wall of diverticulum (*white arrow*). Histolology revealed squamous cell carcinoma

References

1. Dalrymple NC, Casford B, Raiken DP, Elsass KD, Pagan RA. Pearls and pitfalls in the diagnosis of ureterolithiasis with unenhanced helical CT. Radiographics. 2000;20:439–47.
2. Lawler LP, Jarret TW, Corl FM, Fishman EK. Adult ureteropelvic junction obstruction: insights with three-dimensional multi-detector Row CT. Radiographics. 2005;25:121–34.
3. Rouviere O, Lyonnet D, Berger P, Pangaud C, Gelet A, Martin X. Ureteropelvic junction obstruction: use of helical CT for preoperative assessment–comparison with intraarterial angiography. Radiology. 1999;213:668–73.
4. Lau PHC, McKenzie AF. Megacalycosis revisted. J HK Coll Radiol. 2002;5:109–10.
5. Kimche D, Lask D. Megacalycosis. Urology. 1982;19(5):478–81.
6. Rathaus V, Konen O, Werner M, Shapiro Feinberg M, Grunebaum M, Zissin R. Pyelocalyceal diverticulum: the imaging spectrum with emphasis on the ultrasound features. BJR. 2001;74:595–601.
7. Kambadkone AR, Eisner BH, Catalano OA, Sahani DV. New and evolving concepts in the imaging and management of urolithiasis: urologists' perspective. Radiographics. 2010;30:603–23.
8. Loitman BS, Chiat H. Ureteritis cystica and pyelitis cystica. Radiology. 1957;68:345–51.
9. Baumgartner BR, Alagappian R. Malakoplakia of the ureter and bladder. Urol Radiol. 1990;12(3):157–9.
10. Harvin HJ. Ureteral fibroepithelial polyp on MDCT urography. AJR Am J Roentgenol. 2006;187:W434–5.
11. Liddell RM, Reinberger E, Schofield DE, Pelman RS. Fibroepithelial polyp of the ureter in a child. AJR Am J Roentgenol. 1991;157:1273–4.
12. Wong JJ, Wagner BJ, Davis CJ. Transitional cell carcinoma of the urinary tract: radiologic-pathologic correlation. Radiographics. 1998;18:123–42.
13. Winalski CS, Lipman JC, Tumeh SS. Ureteral neoplasms. Radiographics. 1990;10:271–83.
14. Prando A, Prando P, Prando D. Urothelial cancer of the renal pelvicalyceal system: unusual imaging manifestations. Radiographics. 2010;30:1553–66.

15. Browne RFJ, Meehan CP, Colville J, Power R, Torreggiani WC. Transitional cell carcinoma of the upper urinary tract: spectrum of imaging findings. Radiographics. 2005;25:1609–25.
16. Cronin CG, Lohan DG, Blake MA, Roche C, McCarthy P, Murphy JM. Retroperitoneal fibrosis: a review of clinical features and imaging findings. AJR Am J Roentgenol. 2008;191:423–31.
17. Heckmann M, Uder M, Kuefner MA, Heinrich MC. Ormond's disease or secondary retroperitoneal fibrosis? An overview of retroperitoneal fibrosis. Röfo. 2009;181(4):317–23.
18. Connor SEJ, Umaria N, Guest PJ. Extranodal peripelvic and periureteric lymphoma – demonstration with computed tomography. Clin Radiol. 2001;56(5):422–4.
19. Woodward PJ, Sohaey R, Mezzetti TP. Endometriosis: radiologic-pathologic correlation. Radiographics. 2001;21:193–216.
20. Stepniewska A, Grosso G, Molon A, Caleffi G, Perin E, Scioscia M, Mainardi P, Minelli L. Ureteral endometriosis: clinical and radiological follow-up after laparoscopic ureterocystoneostomy. Hum Reprod. 2001;26(1):112–6.
21. Berrocal T, Lopez-Pereira P, Arjonilla A, Gutierrez J. Anomalies of the distal ureter, bladder, and urethra in children: embryologic, radiologic, and pathologic features. Radiographics. 2002;22: 1139–64.
22. Wasserman NF, Zhang G, Posalaky IP, Reddy PK. AJR Am J Roentgenol. 1991;157:69–72.
23. Wasserman NF, La Pointe S, Posalaky I. Ureteral pseudodiverticulosis. Radiology. 1985;155:561–6.
24. Fernbach SK, Feinstein KA, Spencer K, Lindstrom CA. Ureteral duplication and its complications. Radiographics. 1997;17: 109–27.
25. Uthappa MC, Anthony D, Allen C. Retrocaval ureter: MR appearances. Br J R. 2002;75:177–9.
26. Hakenberg OW, Linne C, Manseck A, Wirth MP. Bladder wall thickness in normal adults and men with mild lower urinary tract symptoms and benign prostatic enlargement. Neurourol Urodyn. 2000;19(5):585–93.
27. Nejmeddine A, Atef B, Youssef D, Ramez B, Issam BM. Emphysematous cystitis of the diabetic patient. North Am J Med Sci. 2009;1:114–6.
28. Schistosomiasis. World Health Organization. Available online: http://www.who.int/topics/schistosomiasis/en/. Accessed 6 Nov 2011.
29. Jorulf H, Lindstedt E. Urogenital schistosomiasis: CT evaluation. Radiology. 1985;157:745–9.
30. Evans RJ. Pathophysiology and clinical presentation of interstitial cystitis. Adv Stud Pharm. 2005:8–14.
31. Wong JJ, Woodward PJ, Manning MA, Sesterhenn IA. Neoplasms of the urinary bladder: radiologic-pathologic correlation. Radiographics. 2000;26:553–80.
32. Cancer Facts and Figures 2005. American Cancer Society. Available online: http://www.cancer.org/Research/CancerFactsFigures/cancer-facts-figures-2005. Accessed 6 Nov 2011.
33. Wong JT, Wasserman NF, Padurean AM. Bladder squamous cell carcinoma. Radiographics. 2004;24:855–60.
34. Wong JJ, Woodward PJ, Manning MA, Davis CJ. Inflammatory and nonneoplastic bladder masses: radiologic-pathologic correlation. Radiographics. 2006;26:1847–68.
35. Matta EJ, Kenney AJ, Barre GM, Vanlangendonck RM. Intradiverticular bladder carcinoma. Radiographics. 2005;25: 1397–403.
36. Yu JS, Kim KW, Lee HJ, Lee YJ, Yoon CS, Kim MJ. Urachal remnant diseases: spectrum of CT and US findings. Radiographics. 2001;21:451–61.